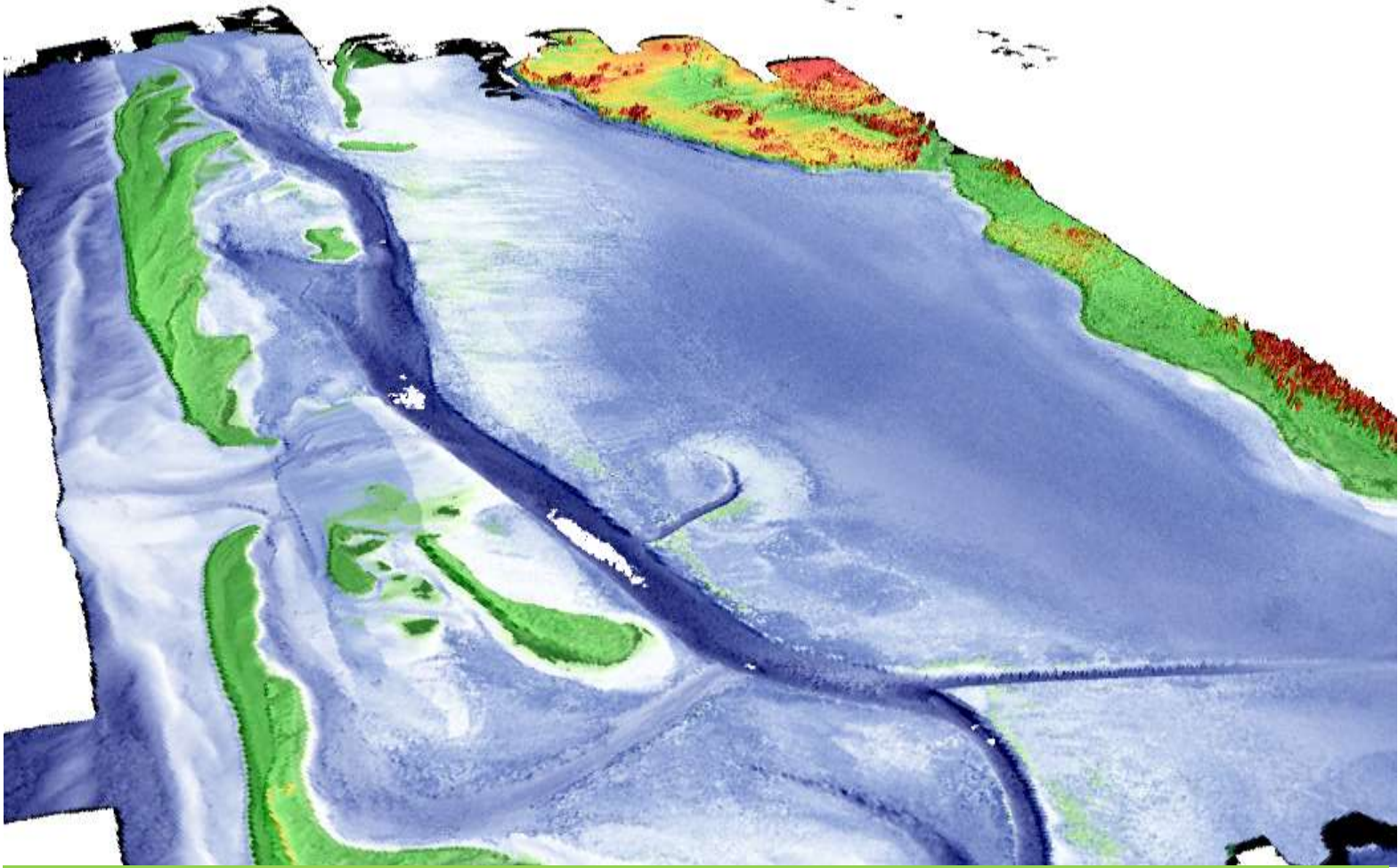


# Tabusintac 2014 Topo-Bathymetric Lidar & Eelgrass Mapping Report



*Prepared by*

Tim Webster, PhD  
Kate Collins, Nathan Crowell, Kevin  
McGuigan, Candace MacDonald  
Applied Geomatics Research Group  
NSCC, Middleton  
Tel. 902 825 5475  
email: [tim.webster@nsc.ca](mailto:tim.webster@nsc.ca)

*Submitted to*

Public Works Government  
Services Canada

January, 2015

## How to cite this work and report:

Webster, T., McGuigan, K., Crowell, N., Collins, K., MacDonald, C. 2014. Tabusintac 2014 Topo-Bathymetric Lidar & Eelgrass Mapping Report. Technical report, Applied Geomatics Research Group, NSCC Middleton, NS.

## Copyright and Acknowledgement

The Applied Geomatics Research Group of the Nova Scotia Community College maintains full ownership of all data collected by equipment owned by NSCC and agrees to provide the end user who commissions the data collection a license to use the data for the purpose they were collected for upon written consent by AGRG-NSCC. The end user may make unlimited copies of the data for internal use; derive products from the data, release graphics and hardcopy with the copyright acknowledgement of **“Data acquired and processed by the Applied Geomatics Research Group, NSCC”**. Data acquired using this technology and the intellectual property (IP) associated with processing these data are owned by AGRG/NSCC and data will not be shared without permission of AGRG/NSCC.

# PWGSC Bathymetric Lidar Report – Tabusintac, NB

---

## Executive Summary

An airborne topo-bathymetric lidar survey was undertaken at Tabusintac, New Brunswick on September 26, 2014. The sensor used was a Chiroptera II integrated topographic bathymetric lidar sensor equipped with a 60 megapixel multispectral camera. Strong winds along the Northumberland Strait during the week of the planned survey reduced water clarity and delayed the surveys at Tabusintac, but good data were collected on Sept. 26. The aircraft required ground-based high precision GPS data to be collected during the lidar survey in order to provide accurate positional data for the aircraft. The coordinates of a Canadian Hydrographic Benchmark monument were supplied to us and used to establish the GPS base station on Sept. 26. The horizontal coordinates were supplied as UTM NAD83 and the vertical elevation was referenced to the local chart datum. A Leica GS14 base station was set up over the monument and logged at 0.5 sec intervals during the survey. Some RTK GPS validation data were collected along the deck of the wharf and parking lot to compare to the topographic lidar returns. Lidar elevation comparison around the wharf indicate a difference between the survey RTK GPS measurements and the lidar of a mean of -5 cm with a standard deviation of 2 cm for 37 points. Boat-based ground truth data collection occurred on Sept. 26 during the lidar survey in a 15 foot aluminum boat. Ground truth surveys included water clarity measurements using a Secchi disk, depth validation measurements using an echo sounder and a lead ball on a rope, underwater photographs of the seabed using a GoPro camera, and GPS measurements using a handheld GPS unit. The depths were used in addition to the lidar derived water surface to calculate the seabed elevation and compared to that derived from the lidar data. The difference in elevation between the 18 manual ground truth points and the lidar was a mean of -7.5 cm with a standard deviation of 26 cm. The ground truth photographs were used in post-processing to provide information on seabed type, such as sand, rock, or eelgrass. We were supplied with two additional ground truth datasets from Department of Fisheries and Oceans and PWGSC; the latter dataset was acquired by Stantec Consulting. The lidar data were processed in Lidar Survey Studio, a proprietary software that accompanies the Chiroptera II sensor, and classed into ground (includes trees and buildings), water surface, and bathymetric points that were used to produce a Digital Elevation Model (DEM) for the study area. Maps of lidar intensity data were also produced; these show information on the seabed cover type and were used in part with the lidar returns to produce an eelgrass distribution map. The aerial photos were processed into an orthophoto mosaic at 20 cm resolution. Various lidar elevation derivative maps were constructed and a method developed to map the distribution of eelgrass. A presence – absence map was constructed for eelgrass from the lidar data and compared to the combined ground truth data. Results indicate 80% agreement between the 69 ground truth points and the lidar derived eelgrass map. We consider the analysis of lidar to map the seabed cover, for example eelgrass, an area of active research and anticipate improvements to our method of classification in the future. Overall, the lidar sensor operated very well in this environment and was able to acquire bathymetric data for the entire study area.

## Table of Contents

Executive Summary.....	ii
Table of Contents.....	iii
Table of Figures.....	iv
List of Tables.....	vi
1 Introduction.....	1
2 Methods.....	4
2.1 Sensor Specifications and Installation.....	4
2.2 Lidar Survey Details.....	6
2.3 Meteorological Conditions.....	9
2.4 Ground Truth Data Collection.....	10
2.5 Lidar Data Processing.....	14
2.5.1 Point Cloud Processing.....	14
2.5.2 Gridded Surface Models.....	18
2.5.3 Aerial Photo Processing.....	18
2.5.4 Lidar Validation.....	19
2.5.5 Eelgrass Mapping.....	19
3 Results.....	20
3.1 Lidar Point Cloud Features.....	20
3.2 Lidar Surface Models.....	20
3.2.1 Intensity-Reflectance Data.....	21
3.3 Orthophotography.....	26
3.4 GPS Data and Lidar Validation.....	29
3.5 Eelgrass map.....	34
4 Conclusions.....	40

# PWGSC Bathymetric Lidar Report – Tabusintac, NB

## Table of Figures

Figure 1: The study area shows new photography of the barrier islands that define the outer area of Tabusintac Bay. The lidar area included McEachern’s Point wharf and the gullies 3, 4 and 5. Map supplied by PWGSC. ....	3
Figure 2 Principals of topo-bathymetric lidar. The system utilizes two lasers, a near infrared and a green laser to surface the land and marine topography. ....	5
Figure 3: (a) Aircraft used for September 2014 lidar survey; (b) display seen by lidar operator in-flight; (c) main body of sensor (left) and laser pointing through a hole cut in the bottom of the plane (right); (d) large red circles are the lasers; the RCD30 lens (right) and low resolution camera (left). ....	5
Figure 4 Planned flight lines (yellow lines) and photo capture events (green dots). GPS checkpoint used for validation are also shown in red triangles. ....	6
Figure 5 Sketch of the CHS benchmark 88B9004 supplied by PWGSC to be used for GPS base station. ....	7
Figure 6 GPS base setup over CHS benchmark 88B9004. Note the memorial built on the guard rail for the fisherman who died after they ran aground in 2013. ....	8
Figure 7 Survey grade GPS base station for aircraft trajectory and RTK check points. ....	8
Figure 8: Wind speed (top panel) and direction (middle panel, where the wind is blowing from the direction shown) from Environment Canada weather station at Miramichi, NB. The lower panel shows vectors representing the direction the wind is blowing towards. Note the lower wind speeds proceeding and during the lidar flight on Sept. 26. ...	10
Figure 9 Example of a Secchi disk used to measure water clarity during the lidar survey. Panel A is the secchi disk with graduated rope. Panel B is the disk lowered in the water until it cannot be seen. Panel C is an AGRG researcher deploying the disk. Panel D is an AGRG researcher using the lead ball for a depth measurment. ....	11
Figure 10 Example of the 1 m by 1 m quadrat used to photograph the seabed. Panel A shows the quadrat on its side in the boat. Panel B shows it submerged. Panel C shows an example of eelgrass. Panel D and E show quadrat photos of eelgrass from top and side cameras. Panel D and E show quadrat photos of eelgrass with algae from top and side cameras. ....	12
Figure 11 AGRG RCD430 true colour orthophoto mosaic of Tabusintac Bay with eelgrass grout truth survey locations. ...	13
Figure 12 Swath coverage of lidar flight lines acquired for Tabusintac. The survey was flown with 30% overlap. ....	14
Figure 13 Example of LSS where the lidar points coloured by elevation and a cross-section extracted across the channel between the two outer dunes. Panel below represents the cross-section where the points are coloured by class; brown is ground, blue is bathymetry, and red is the computed water surface. ....	15
Figure 14 Example of LSS waveforms. The background image represents the lidar points in greyscale representing the green laser reflectance and the cross-section at the channel. The cross section of the classified point is in the lower panel. The right panel is the waveform of the water surface (red vertical line) and seabed (blue line). ....	16

# PWGSC Bathymetric Lidar Report – Tabusintac, NB

---

<b>Figure 15: Example of multiple frames (56, 57, and 58) from multiple flight lines (008 on top and 009 below) of the GPS base station location at Little Harbour after orthorectification. The green dots are GPS locations along the parking lot rail and the aircraft control benchmark on the ground below the tripod where the bottom of the legs are represented by the green diamond. ....</b>	<b>19</b>
Figure 16 Example of the green lidar seabed reflectance. High values of reflectance indicate more light is being reflected (less light being absorbed, e.g. bright materials), and low values indicate less light is being reflected (more light being absorbed, e.g. dark materials). Note that this map of reflectance has not been normalized for depth. ....	21
Figure 17 Lidar derived bathymetric map, elevations referenced to chart datum. ....	22
Figure 18 Colour shaded relief map of Tabusintac. ....	24
Figure 19 Colour shaded relief with intensity-reflectance map of Tabusintac.....	25
Figure 20 True colour composite of the Tabusintac orthophoto mosaic. ....	27
Figure 21 Colour NIR composite of the orthophoto mosaic of Tabusintac. ....	28
Figure 22 Example of the density of the lidar points, topo laser (yellow dots) and the hydro laser (green triangles) with the RTK GPS check points (red triangles). The inset in the lower left corner is a zoom to show the point distribution in detail. ....	30
Figure 23 DEM derived from the topo laser at 2 m grid cells with the RTK GPS checkpoints overlaid (red triangles). The labels indicate the difference in elevation between the GPS and lidar DEM in metres.....	31
Figure 24 Histogram of the difference in elevation, DZ, between the GPS checkpoints and the lidar DEM. The mean difference of -0.05 m with a standard deviation of 0.02 m. ....	32
Figure 25 Tabusintac seabed elevation validation. The difference in elevation between the ground truth manual measurements and the lidar elevation is presented in metres as DZ_m_DEM. ....	33
Figure 26 Eelgrass probability map, darker green indicates a higher probability of eelgrass occurrence. ....	35
Figure 27 Eelgrass probability map with ground truth, eelgrass presence is a blue dot, absence is a red triangle.....	36
Figure 28 Presence-absence eelgrass map derived from lidar with ground truth (red triangle, blue dot) and where the ground truth matches the map (yellow circles).....	37
Figure 29 Orthophoto on the left of the dredged channel with ground truth points that agree with the map. Right is the orthophoto with lidar derived eelgrass (green) and ground truth points.....	38
Figure 30 Orthophoto on the left of the main channel and opening with ground truth points that agree with the map. Right is the orthophoto with lidar derived eelgrass (green) and ground truth points. ....	39
Figure 31 Orthophoto on the left of the southern channel with ground truth points that agree with the map. Right is the orthophoto with lidar derived eelgrass (green) and ground truth points.....	40

# PWGSC Bathymetric Lidar Report – Tabusintac, NB

---

## List of Tables

Table 1 Coordinates supplied by PWGSC for CHS benchmark for GPS control. ....	7
<b>Table 2 Table of delivered LAS classes combining the hydro (HD) and topo (TD) lidars. ....</b>	<b>17</b>
Table 3 Computed projection and geodetic coordinates of CHS benchmark.....	29

## 1 Introduction

The requirement for accurate and detailed information along Canada’s coastal zone is imperative in order to protect existing and plan for future infrastructure, and to make sound decisions with regard to activities that support economic development. Recently the Applied Geomatics Research Group (AGRG) at the Nova Scotia Community College (NSCC) acquired a topographic-bathymetric (topo-bathy) lidar sensor and high resolution aerial camera that is capable of surveying the land elevations and the submerged coastal topography. The ability of an airborne sensor to accurately survey the near shore bathymetry (submerged elevation) offers an opportunity to produce detailed information across the land-sea boundary in an area that has traditionally not been mapped because of the expense and limitations of traditional mapping technologies (air photos on land and boats and echo sounders on the water).

The lidar system utilizes lasers mounted in an aircraft to precisely measure the topography surrounding coastal waters and also sees through the water to measure the bathymetry. The reflection of the green laser from the seabed can be used to also map the seabed cover including submerged vegetation, for example eelgrass, which is often used by regulators, such as Fisheries and Oceans Canada (DFO), as a measure of ecosystem health. These data can be used to capture the state of the seabed and aquatic vegetation and act as a quantitative baseline prior to any future coastal developments. The lidar sensor is coupled with a high resolution aerial camera (Leica RCD30) which is capable of collecting traditional true colour images (red, green, and blue or RGB) and also a near-infrared (NIR) image which is highly sensitive to the existence of vegetation, such as exposed seaweed in the coastal zone. The ability of the lidar sensor to acquire detailed elevation data on land and continuously into the submarine environment provides information that can be used, for the land areas, to assess risk of coastal flooding, erosion and geohazards. For the intertidal and sub tidal areas this level of information has never been surveyed and provides details for updates for navigation to accurately map the channel for safe passage for small craft harbours.

The Tabusintac Bay study area (Figure 1) was surveyed on September 26, 2014 in the afternoon. The survey was funded by Public Works and Government Services Canada (PWGSC) and two main deliverables: a digital elevation model (DEM) of the bathymetry, and a map of eelgrass distribution within the bay. Tabusintac Bay is a shallow, flat bay with dynamic sand spit barriers and a deep channel. The most recently formed gully (Figure 1, area 4, South Channel) is used by fishers to access the Northumberland Strait, and requires dredging to keep the sediment from filling in the channel. In May of 2013 three fishermen drowned at the site when their boat hit a sandbar and began taking on water. An accurate DEM of the bathymetry of Tabusintac Bay will allow managers to dredge the channel most effectively and efficiently to provide a safely navigable passage for fishers and recreational boaters. The second deliverable is an eelgrass map that will indicate eelgrass distribution with depth throughout the bay. Eelgrass plays an important biophysical role in the health of ecosystems and is widely accepted as an indicator of overall ecosystem health, but is experiencing some declines in the Southern Gulf of St Lawrence. Eelgrass is often used by regulators, such as DFO, as a measure of ecosystem health, but an efficient method of mapping eelgrass is required to enable eelgrass to be monitored through time. Bathymetric lidar

## PWGSC Bathymetric Lidar Report – Tabusintac, NB

---

provides the opportunity to conduct repeat surveys to map the changes in both bathymetry and eelgrass distribution over time.

This report provides details on fieldwork and instrumentation in the Methods section, including details on the Chiroptera II lidar sensor used for the surveys (Section 2.1), the ancillary data collected on the ground during the lidar flights (Section 2.4), and the data processing methods (Section 2.5). The Results section includes maps of bathymetry, reflectance, and eelgrass coverage.



Figure 1: The study area shows new photography of the barrier islands that define the outer area of Tabusintac Bay. The lidar area included McEachern's Point wharf and the gullies 3, 4 and 5. Map supplied by PWGSC.

## 2 Methods

### 2.1 Sensor Specifications and Installation

The lidar sensor is a Chiroptera II integrated topographic bathymetric lidar sensor equipped with a 60 megapixel multispectral camera. The system incorporates a 1064 nm near infrared laser for topographic (topo) laser for ground returns and a green 532 nm laser for hydrographic (hydro) returns (**Error! Reference source not found.**). The lasers utilize a Palmer scanner, which forms an elliptical pattern with angles of incidence of 14° forward and back and 20° to the sides of the flight track. This enables more returns, lidar coverage from many different angles, on vertical faces, causes less shadow effects in the data, and is less sensitive to ocean wave interaction. The beam divergence of the topo laser is 0.5 mrad and from the hydro laser (green) is 3 mrad. The topo laser can scan with a pulse repetition frequency up to 400 kHz and the hydro laser can scan with a pulse repetition frequency up to 35 kHz. The hydro laser is limited by depth and water clarity, and has a depth penetration rating of approximately 1.5 x the Secchi depth (a measure of turbidity or water clarity). The Leica RCD30 camera collects co-aligned RGB+NIR motion compensated photographs which can be orthorectified and mosaicked into a single image in post-processing, or analyzed frame by frame for maximum information extraction. The RCD30 is a 60MPIX camera with a focal length lens of 53 mm and produces images 6732 by 9000 pixels in the across and along track direction, respectively. The across track field of view is 54°.

AGR-NSCC does not own an aircraft, only the sensor. AGRG partnered with Leading Edge Geomatics to assist in the operations of the survey and arranging the aircraft. A twin engine aircraft was contracted that was certified to carry the Chiroptera II sensor suite and had a hole suitable to house the sensor head. The lidar sensor was installed in the aircraft in Fredericton, NB on Sept. 22. Calibration flights were conducted over Fredericton at altitudes of 400 m and 100 m on Sept. 23. The laser systems and camera were calibrated and aligned with the navigation system which consists of a survey grade GPS mounted on the roof of the aircraft and an inertial measurement unit (IMU) mounted above the laser system (Figure 3.)

The aircraft has a hole cut in the bottom for the laser to face the ground and installation involves fitting the control unit and the sensor head into the hole (Figure 3b). The system also includes a 5 megapixel quality assurance camera that the lidar operator is able to view during the flight, along with the waveform of the returning pulse and the flight plan (Figure 3c). Figure 3d shows the downward facing portion of the sensor head, including the red (topographic) and green (bathymetric) lasers, which shoot and return to the large red circles; the lenses on the left and right are the low and high resolution cameras, respectively.

The sensors were installed in the aircraft on Monday, September 22 (Figure 3a). The aircraft had a hole cut in the bottom for the laser and cameras to image the ground and installation involved fitting the sensor head into the hole (Figure 3c) and the associated control rack on the floor and user display screens on another rack in the aircraft (Figure 3b). Along with the lasers and high resolution camera, the lidar system also includes a 5 megapixel quality assurance camera that the lidar

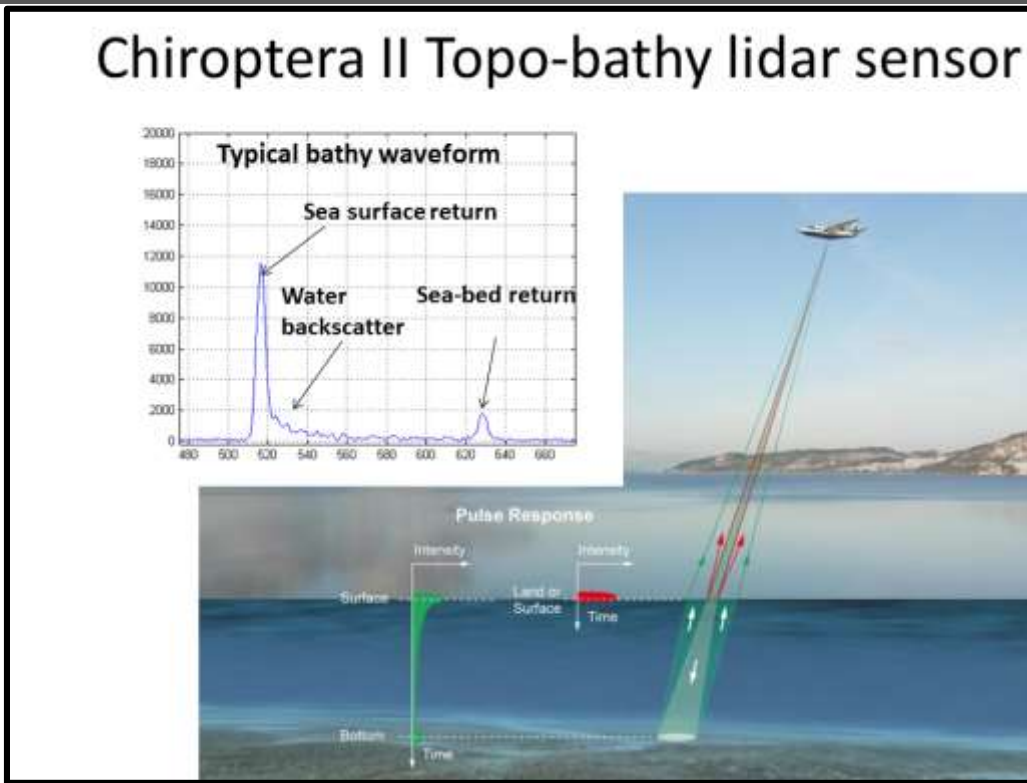


Figure 2 Principles of topo-bathymetric lidar. The system utilizes two lasers, a near infrared and a green laser to surface the land and marine topography.

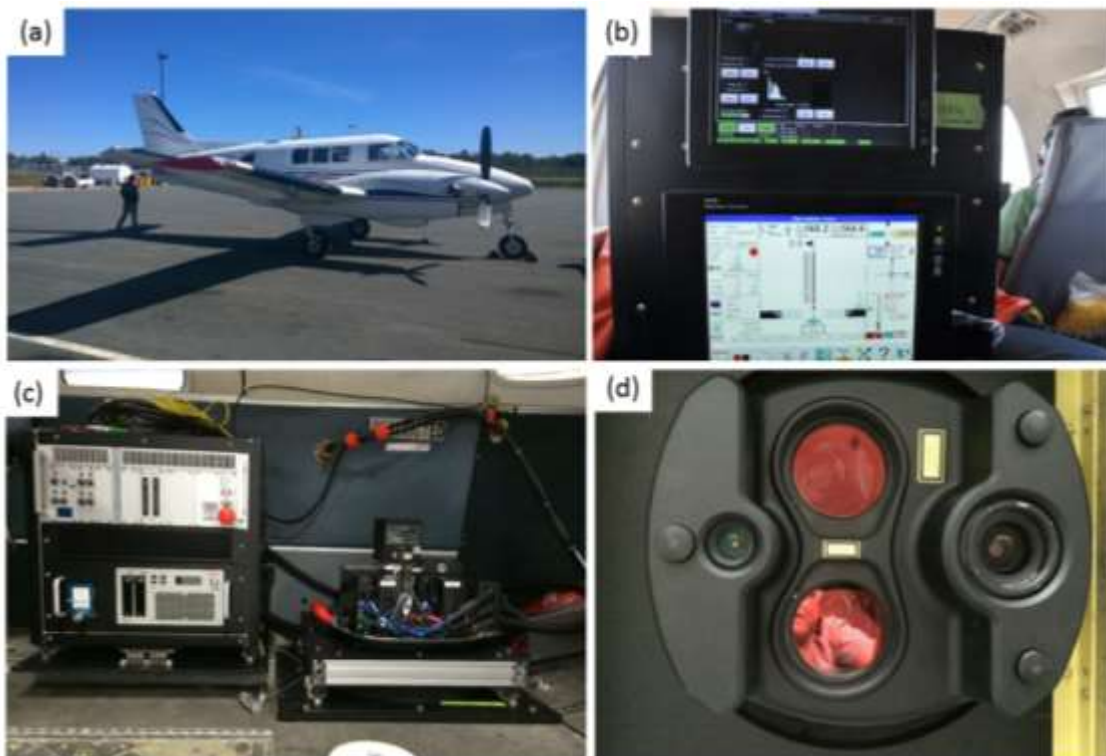


Figure 3: (a) Aircraft used for September 2014 lidar survey; (b) display seen by lidar operator in-flight; (c) main body of sensor (left) and laser pointing through a hole cut in the bottom of the plane (right); (d) large red circles are the lasers; the RCD30 lens (right) and low resolution camera (left).

# PWGSC Bathymetric Lidar Report – Tabusintac, NB

operator is able to view during the flight, along with the waveform of the returning pulse and the flight plan (Figure 3b). Figure 3d shows the downward facing portion of the sensor head, including the red (topographic) and green (bathymetric) lasers, which shoot and return to the large red circles; the lenses on the left and right are the low and high resolution cameras, respectively. During installation the laser systems and camera were calibrated and aligned with the navigation system which consists of a survey grade GPS mounted on the roof of the aircraft and an inertial measurement unit (IMU) mounted above the laser system. Calibration flights were conducted over Fredericton at altitudes of 400 m and 1000 m on Tuesday, Sept. 23, following a wind and rain event on Sept. 22.

## 2.2 Lidar Survey Details

A lidar survey was conducted for Tabusintac on Friday September 26 starting near noon ADT. Low tide at Lower Escuminac was predicted to occur at 12:15 PM ADT on Sept. 26. The survey was planned using Mission pro software at an altitude of 400 m above ground at a flying speed of 140 knots. The planned flight lines and photo events are shown in Figure 4.



Figure 4 Planned flight lines (yellow lines) and photo capture events (green dots). GPS checkpoint used for validation are also shown in red triangles.

# PWGSC Bathymetric Lidar Report – Tabusintac, NB

A Canadian Hydrographic Service control benchmark was supplied by PWGSC to be used to establish the GPS base station for the aircraft. A sketch and description of the monument was supplied along with UTM easting and northing coordinates referenced to UTM Zone 20 NAD83 projection and datum and an elevation referenced to local chart datum (Figure 5) (Table 1).

**Table 1 Coordinates supplied by PWGSC for CHS benchmark for GPS control.**

UTM Easting m NAD83	UTM Northing m NAD83	Elevation m (Chart Datum)
351233.427	5244833.605	3.12

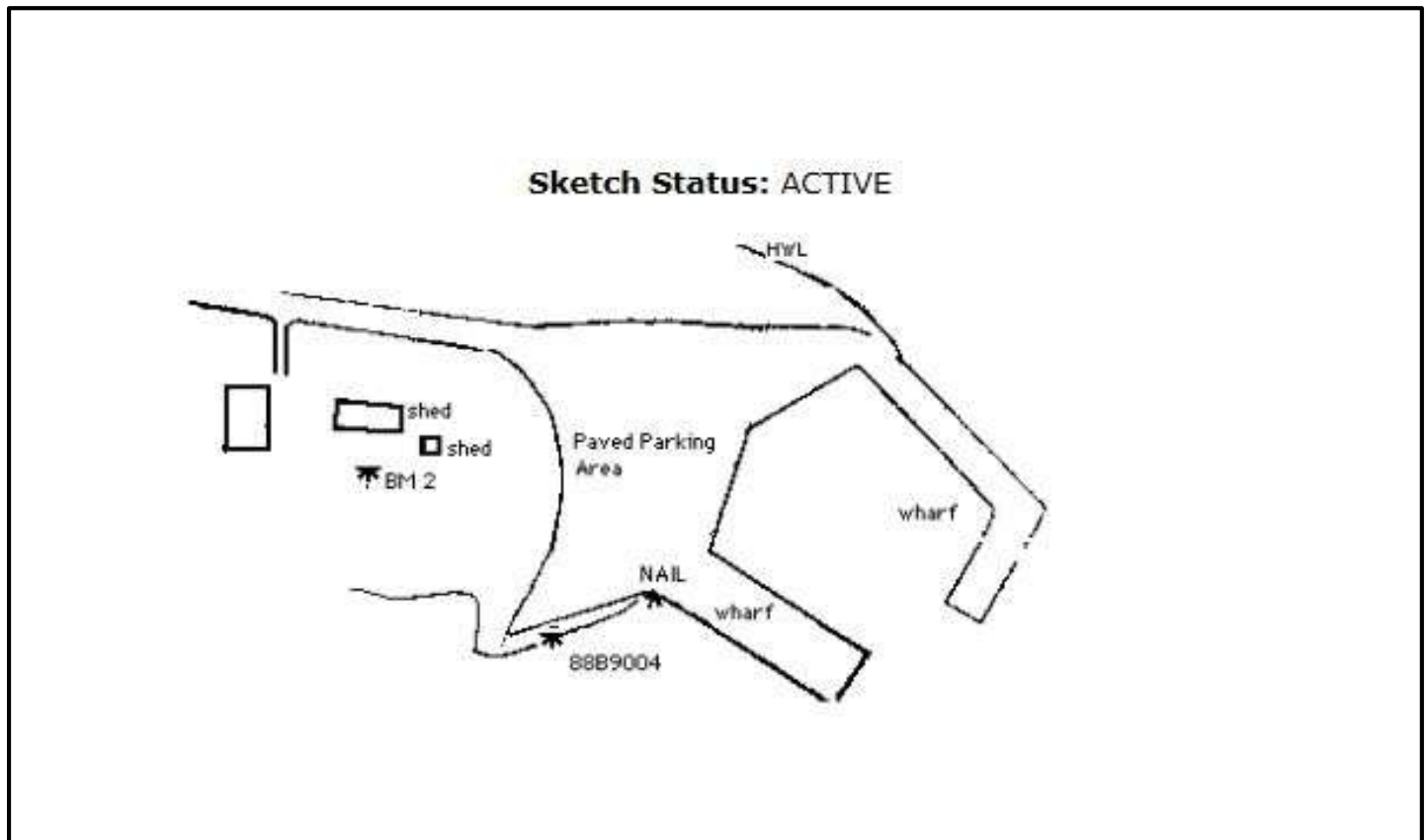


**Figure 5 Sketch of the CHS benchmark 88B9004 supplied by PWGSC to be used for GPS base station.**

The GPS base station was set to log observations at 1 second intervals and the RTK rover was used to collect lidar validation points on hard flat surfaces (Figure 6). These validation points were collected at the parking lot adjacent to the wharf as well as the wharf deck. The survey area was constrained to the coastal areas so there were very few roads that could be used to collect GPS check points to be used for validation (Figure 7). Depth measurements were taken with low precision echo sounders as well as manually using a graduated rope with the Secchi disk. These were measures of depth to the bottom from the water surface and positioned using a code based GPS solution from a Garmin 760, which has a horizontal accuracy of several metres. To compare to the lidar depth, which is measured relative to the chart datum, the water



Figure 6 GPS base setup over CHS benchmark 88B9004. Note the memorial built on the guard rail for the fisherman who died after they ran aground in 2013.



Figure 7 Survey grade GPS base station for aircraft trajectory and RTK check points.

surface was extracted from the lidar for the depth points and used to subtract the manual depths and compared to the DEM.

### **2.3 Meteorological Conditions**

Meteorological conditions during and prior to topo-bathy lidar data collection are an important factor in successful data collection. As the lidar sensor is limited by water clarity, windy weather that stirs up sediment in the seawater can prevent good laser penetration. Rainy weather is not suitable for lidar collection, and the glare of the sun must also be factored in for the collection of aerial photography. The closest weather station to the site is operated by Environment Canada at Miramichi, NB. In addition to checking the current and past conditions, local knowledge of the water clarity is critical. We were assisted by a local oyster fisherman, Eric Thibodeau, who was on the water daily and could tell us the clarity and wind conditions.

Figure 8 shows wind data recorded at Miramichi in the days before the survey and shows a strong northerly wind event on Sept. 23. The wind speed slowed and rotated to the south on the 24<sup>th</sup>, then back to the north on the 25<sup>th</sup> to less than 20 km/hr. Prior to this it was reported that the water in the bay was extremely turbid and the bottom could not be seen visually. Eventually the winds died down, and this gave the water in the bay enough time to clear. However, in the very early morning of the 26<sup>th</sup> the winds exceeded 20 km/hr but died off by late morning and did not cause too much increased turbidity. From noon onward on the 26<sup>th</sup> winds were 10 km/hr or less from the north. They picked up again on the 27<sup>th</sup> and another event of winds greater than 20 km/hr occurred late on the 28<sup>th</sup>.

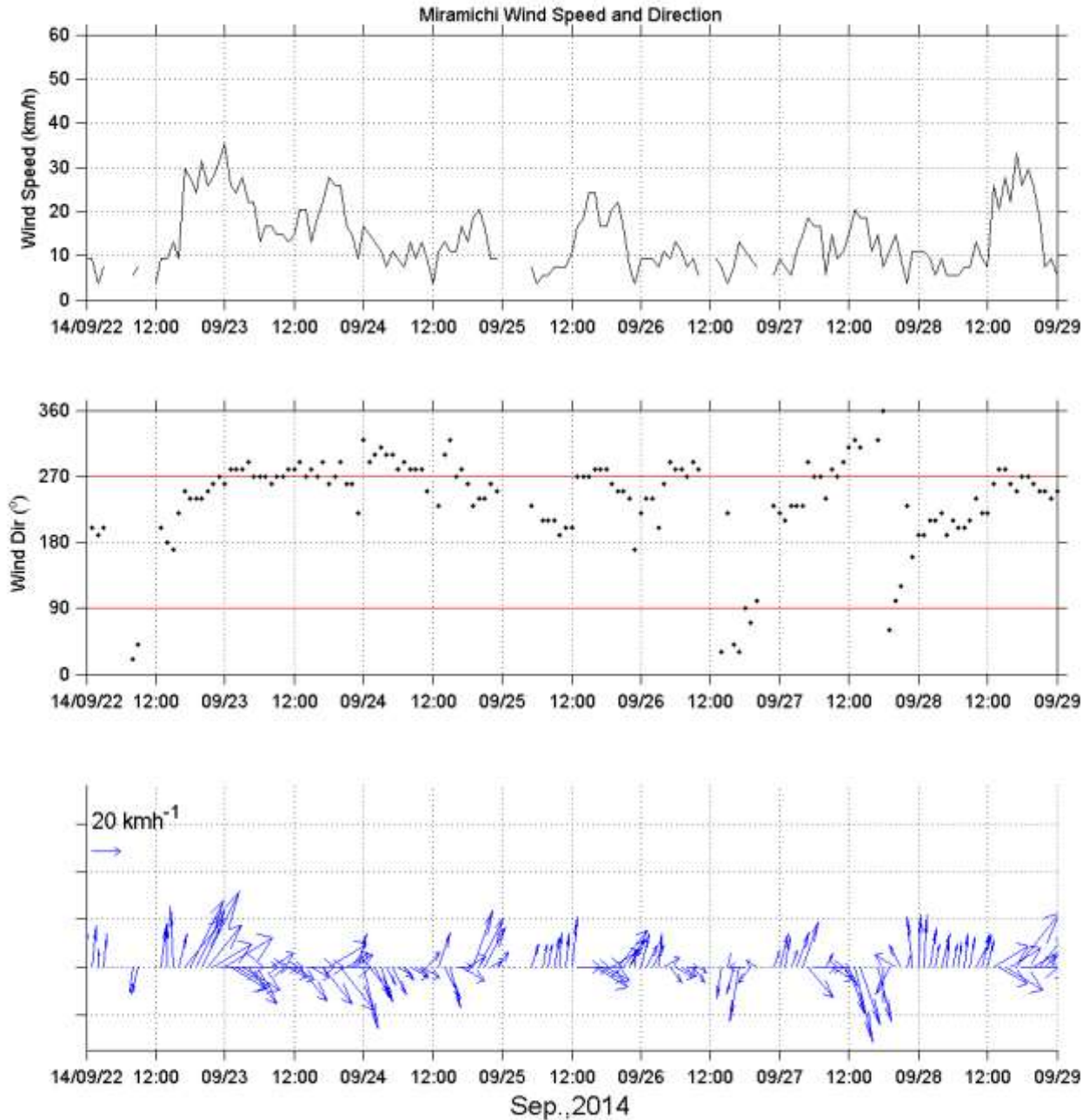


Figure 8: Wind speed (top panel) and direction (middle panel, where the wind is blowing from the direction shown) from Environment Canada weather station at Miramichi, NB. The lower panel shows vectors representing the direction the wind is blowing towards. Note the lower wind speeds preceding and during the lidar flight on Sept. 26.

## 2.4 Ground Truth Data Collection

Ground truth data is another important aspect of topo-bathy lidar data collection. A Humminbird echo sounder with a consumer grade GPS was used to survey the depths within the bay and various point observations were made to sample the water column and bottom conditions. The method consisted of taking a Garmin GPS waypoint, taking a Secchi disk measurement and a depth measurement using a lead ball or the Secchi disk (Figure 9), as well dropping a 1 m by 1 m

## PWGSC Bathymetric Lidar Report – Tabusintac, NB

quadrat over the side equipped with two GoPro cameras to photograph the seabed. One GoPro camera was mounted downward-facing to get a vertical photo and the other mounted facing parallel to the seabed to get a cross section view (Figure 10). Bottom type information is useful for research related to laser returns reflectance, and also for submerged vegetation mapping validation. Scientists from DFO Gulf Region were able get on the water prior to the survey and provide additional ground truth data with respect to eelgrass distribution.

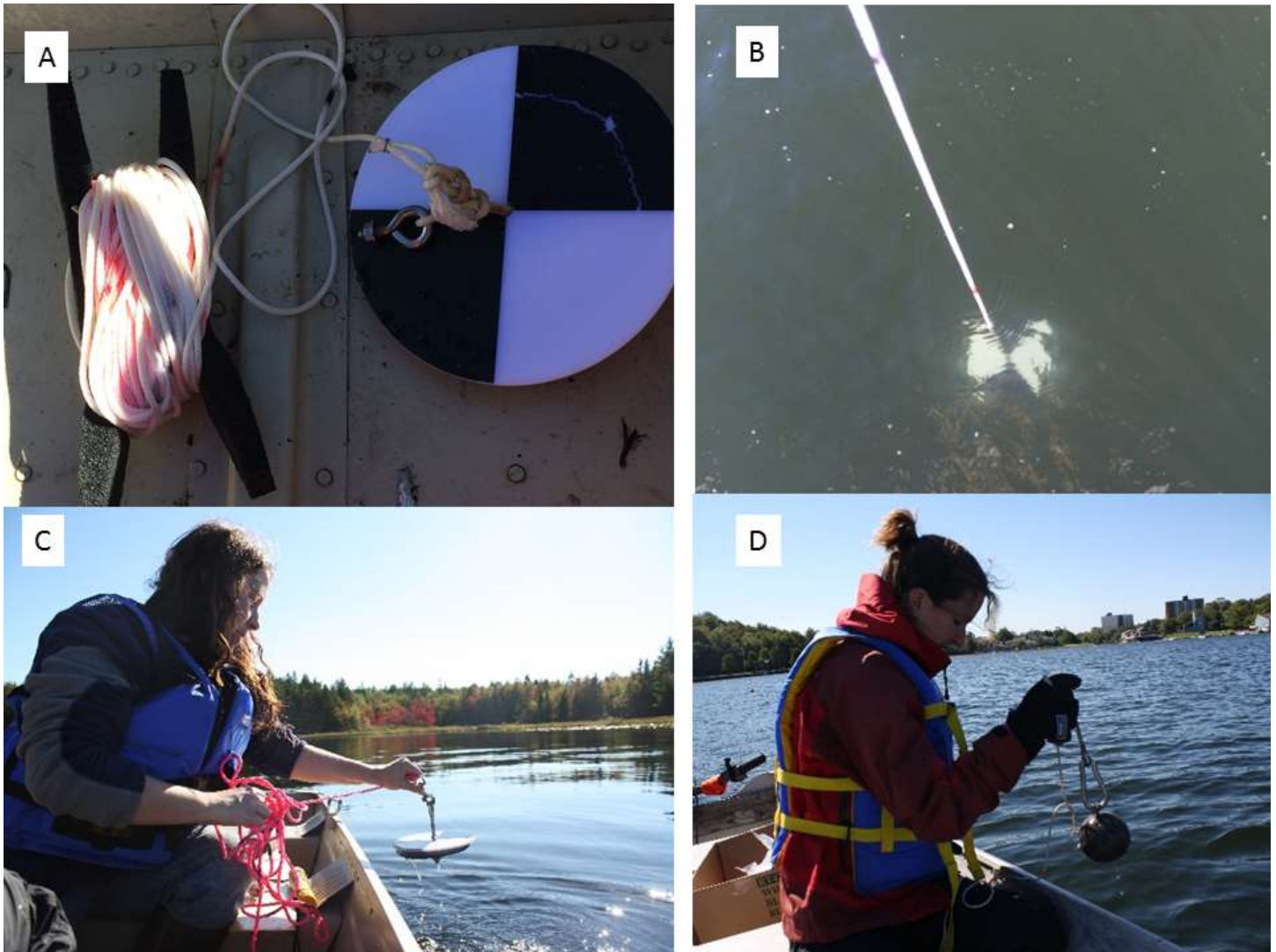


**Figure 9 Example of a Secchi disk used to measure water clarity during the lidar survey. Panel A is the secchi disk with graduated rope. Panel B is the disk lowered in the water until it cannot be seen. Panel C is an AGRG researcher deploying the disk. Panel D is an AGRG researcher using the lead ball for a depth measurement.**

## PWGSC Bathymetric Lidar Report – Tabusintac, NB

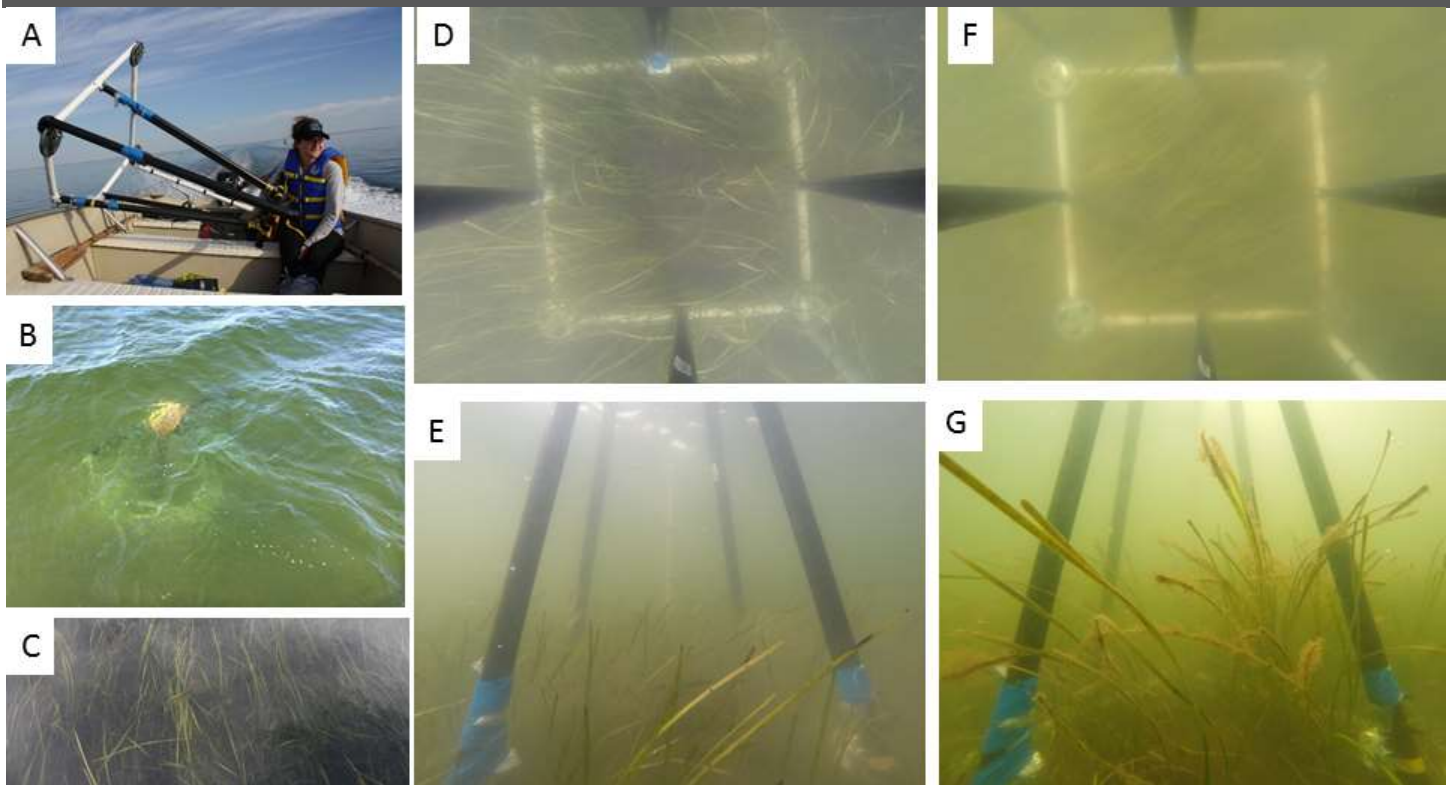


**Figure 10** Example of the 1 m by 1 m quadrat used to photograph the seabed. Panel A shows the quadrat on its side in the boat. Panel B shows it submerged. Panel C shows an example of eelgrass. Panel D and E show quadrat photos of eelgrass from top and side cameras. Panel D and E show quadrat photos of eelgrass with algae from top and side cameras.

As can be seen in the photos in Figure 10 the water clarity was still a bit cloudy on Sept. 26. However, Secchi depth measurements indicated that the disk usually hit the bottom before the disk was no longer visible. The lidar sensor specifications state that the depth penetration is expected to be at least 1.5 times the Secchi depth.

In addition to AGRG conducting a ground truth survey, scientists (Marc Ouellette and Monique Niles) from DFO Gulf Region from Moncton, NB also collected information on eelgrass near the time of the survey. As well Marc Skinner from Stantec Consulting collected ground truth information on eelgrass as part of a study to use World View 2 satellite imagery to map eelgrass in the bay. The location of the ground truth surveys of the three parties is presented in Figure 11 along with the track of the boat used by AGRG during the sampling campaign. The high resolution aerial photos acquired by the RCD30 system, which is part of the Chirptera II lidar sensor have been processed to orthophotos and used to construct a seamless mosaic of the bay which serves as a backdrop to Figure 11.

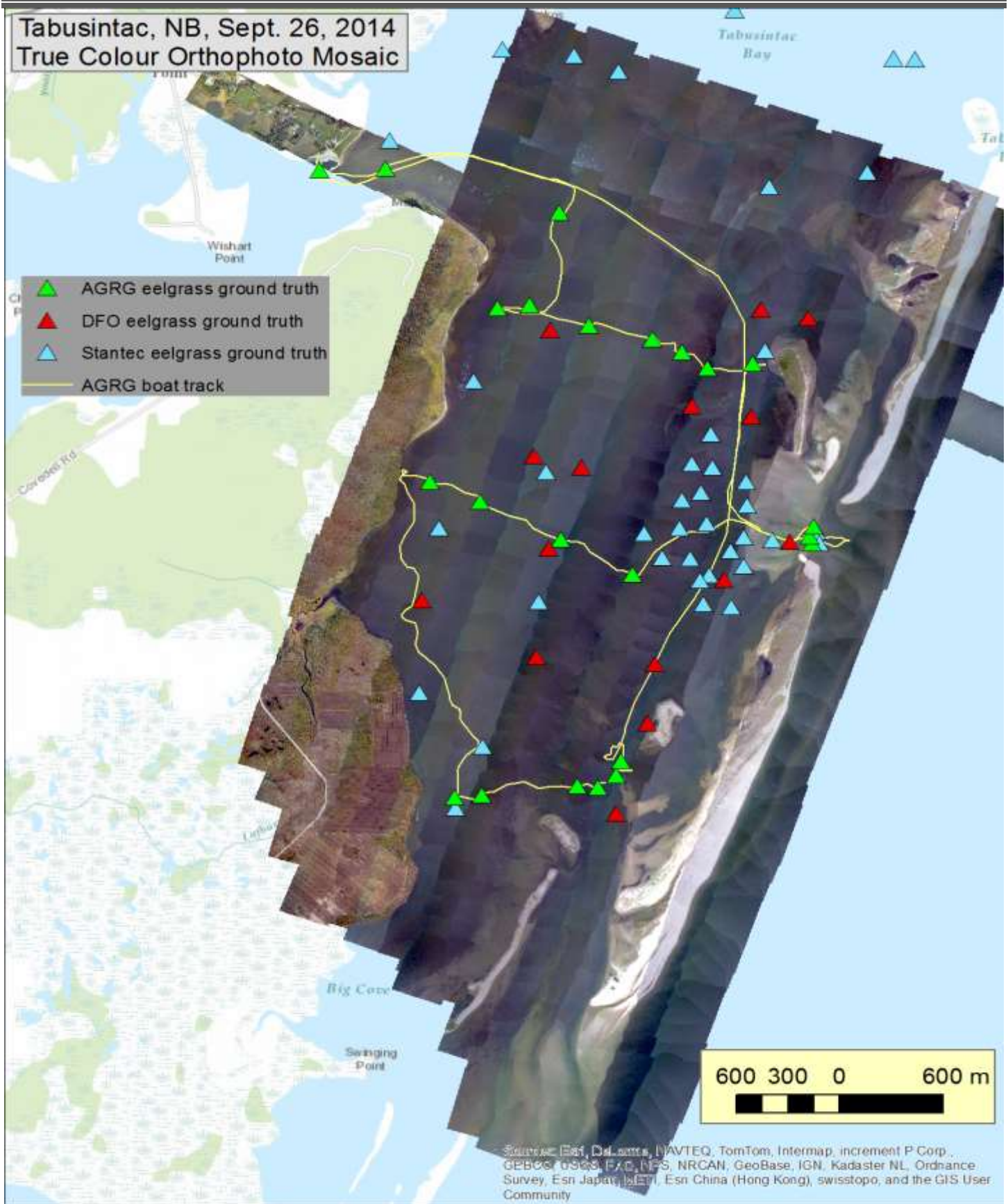
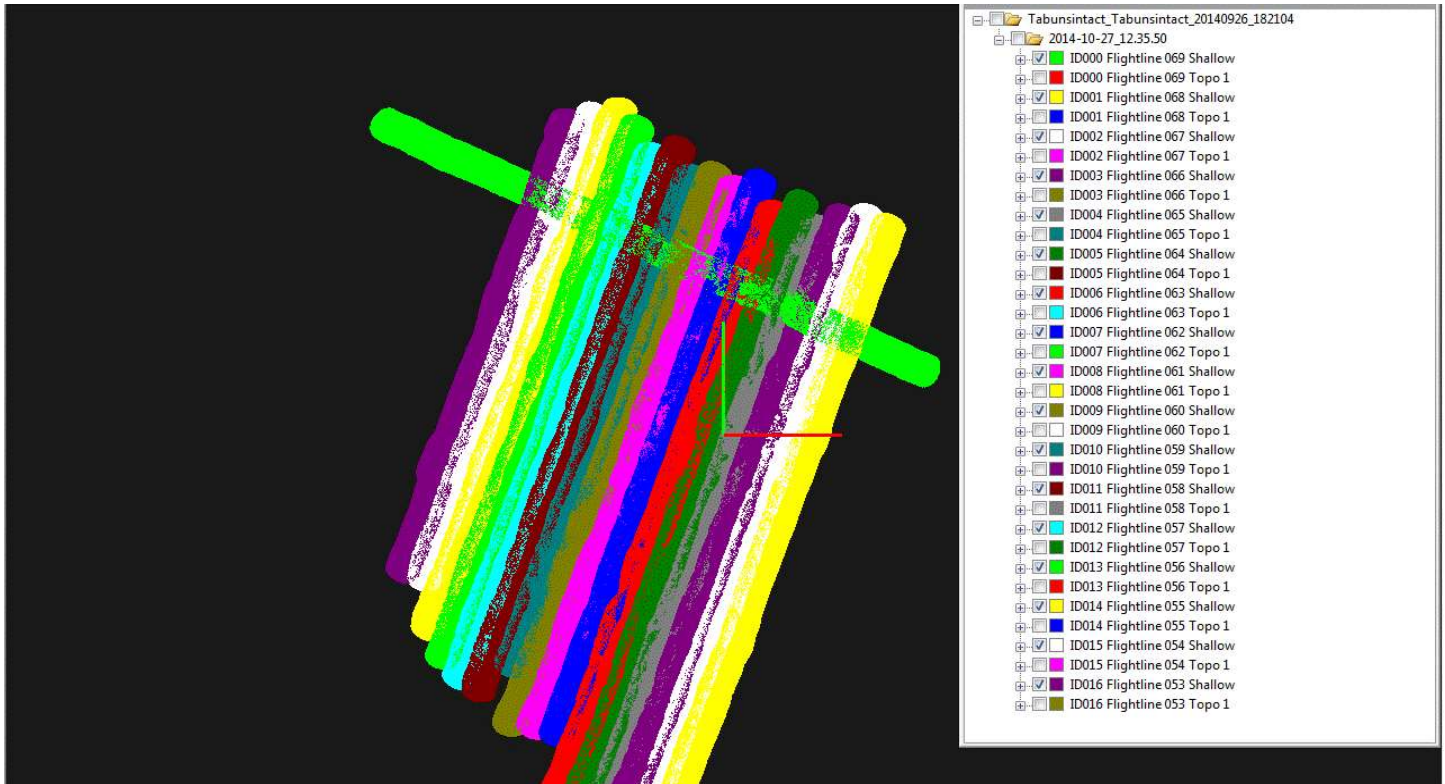


Figure 11 AGRG RCD430 true colour orthophoto mosaic of Tabusintac Bay with eelgrass ground truth survey locations.

## 2.5 Lidar Data Processing

### 2.5.1 Point Cloud Processing

Once the GPS trajectory was processed for the aircraft utilizing the GPS base station and aircraft GPS observations and combined with the inertial measurement unit, the navigation data was linked to the laser returns and georeferenced. Lidar Survey Studio (LSS) software accompanies the Chiroptera II sensor and is used to process the lidar waveforms into discrete points. The data can then be inspected to ensure there was sufficient overlap and no gaps exist in the lidar coverage (Figure 12).



**Figure 12 Swath coverage of lidar flight lines acquired for Tabusintac. The survey was flown with 30% overlap.**

One critical step in the processing of bathymetric lidar is the ability to map the water surface. This is critical for two components of georeferencing the final target or targets that the reflected laser pulse recorded: the refraction of the light when it passes from the medium of air to water and the change in the speed of light from air to water. The LSS software computes the water surface from the lidar returns of both the topo (TD) and hydro (HD) lasers. In addition to classifying points as land, water surface or bathymetry, the system also computes a water surface that ensures the entire area of water surface is covered regardless of the original lidar point density. As mentioned, part of the processing involves converting the raw waveform lidar return time series into discrete classified points using LSS signal processing; points include ground, water surface, seabed, etc. Waveform processing may include algorithms specifically for classifying the seabed through high turbidity water columns, where required. The points can be examined in LSS both in plan view and

## PWGSC Bathymetric Lidar Report – Tabusintac, NB

in cross-section view (Figure 13). The waveforms can be queried for each point so that the location of the waveform peak can be identified and the type of point defined, for example water surface and bathymetry (Figure 14).

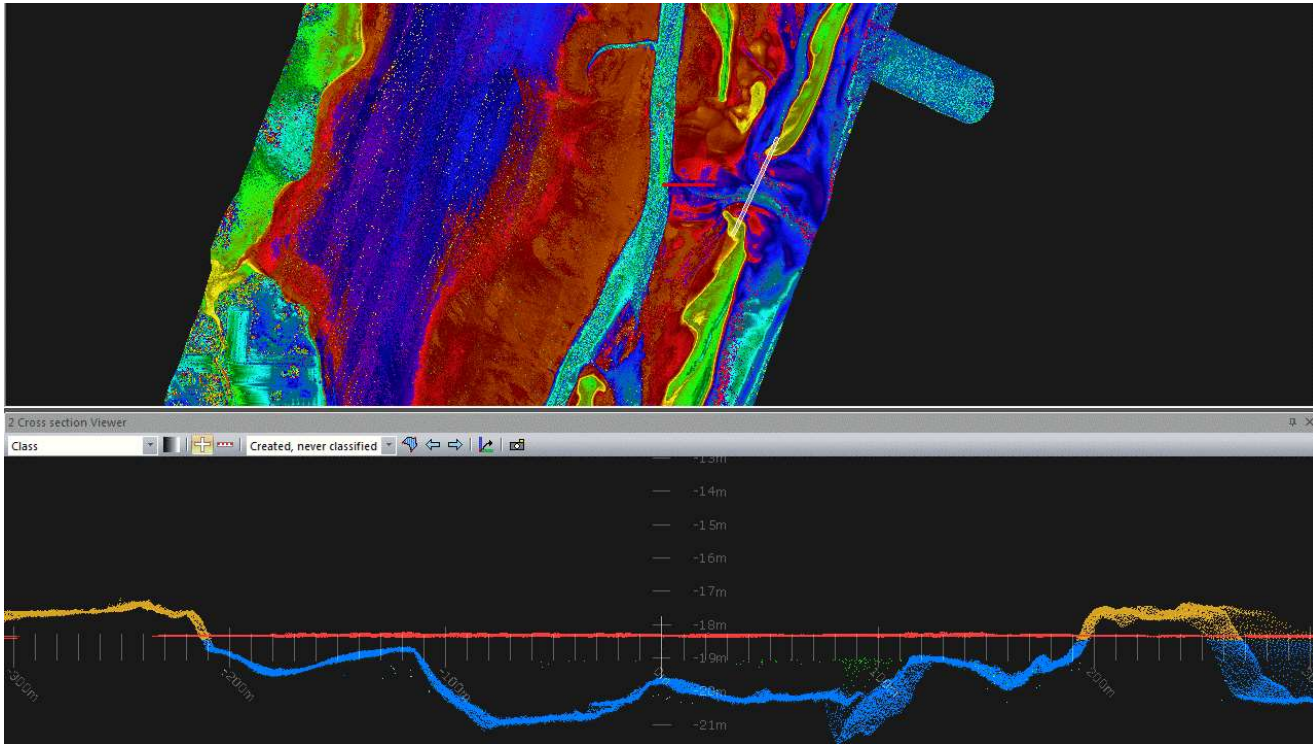


**Figure 13** Example of LSS where the lidar points coloured by elevation and a cross-section extracted across the channel between the two outer dunes. Panel below represents the cross-section where the points are coloured by class; brown is ground, blue is bathymetry, and red is the computed water surface.

## PWGSC Bathymetric Lidar Report – Tabusintac, NB

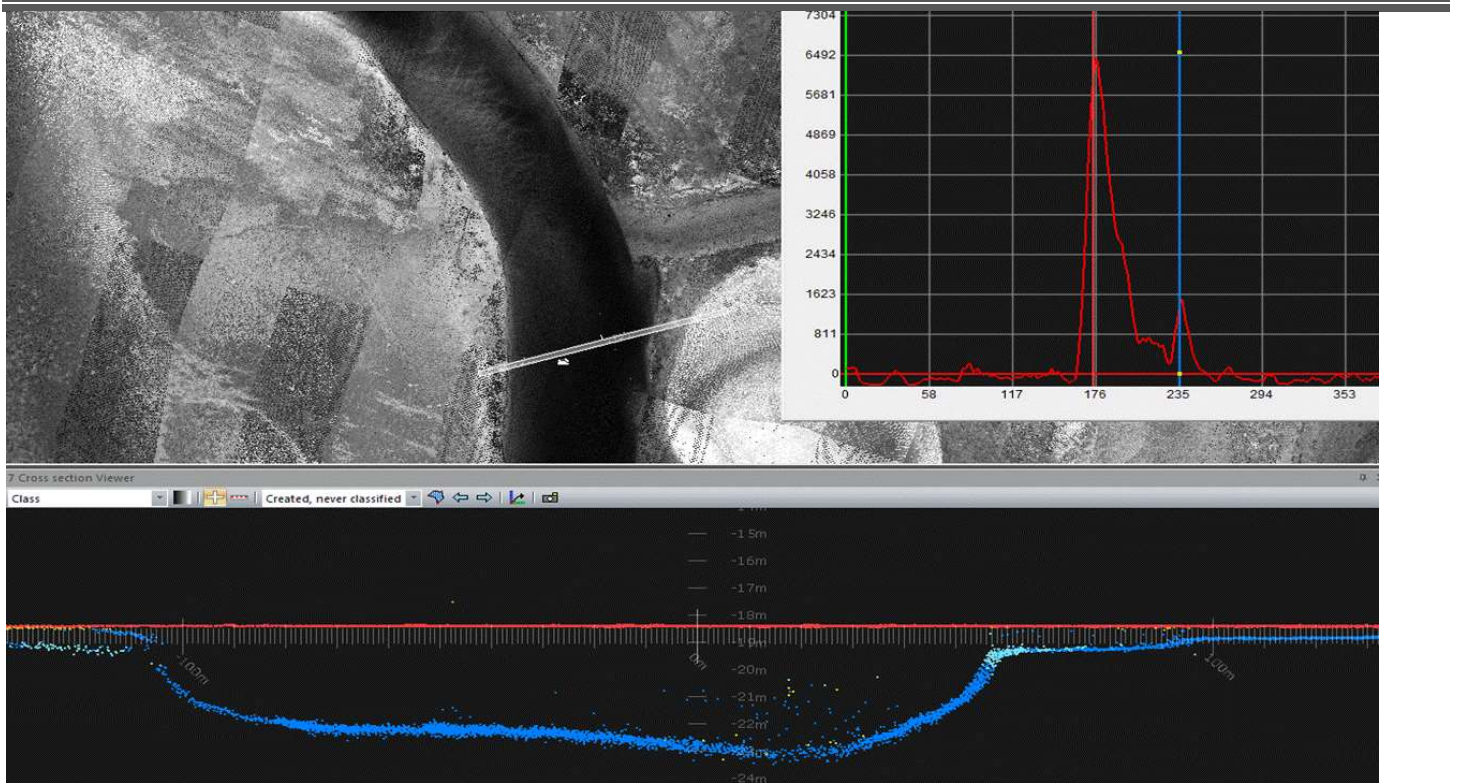


**Figure 14** Example of LSS waveforms. The background image represents the lidar points in greyscale representing the green laser reflectance and the cross-section at the channel. The cross section of the classified point is in the lower panel. The right panel is the waveform of the water surface (red vertical line) and seabed (blue line).

Terrascan was utilized to further classify and filter the lidar point cloud. Because of the differences in the lidar footprint between the TD and HD sensors it was decided that the HD lidar point returns would be used to represent the ocean surface and bathymetry points and the TD lidar points would be used to represent targets above ground. The total point cloud that utilized both sensors was processed in Terrascan where the ground was classified and erroneous points both above and below the ground were defined.

The standard classification numbers used in the LAS format 1.2 do not adequately represent the bathymetric and water surface information, therefore a translation had to be used for the final point cloud. The overlap between flight lines also presented some challenges and it was decided to classify these points separately and code them such that the end user can decide if they want to utilize these points in the surface model construction by coding them uniquely. See Table 2 for the classification codes.

## PWGSC Bathymetric Lidar Report – Tabusintac, NB

Class number	Description
0	Water model
1	Bathymetry (Bathy)
2	Bathy Vegetation
3	N/A
4	Topo laser (TD) Ground
5	TD non-ground (vegetation & buildings)
6	Hydro laser (HD) Ground
7	HD non-ground
8	Water
9	Noise
10	Overlap Water Model
11	Overlap Bathy
12	Overlap Bathy Veg
13	N/A
14	Overlap TD Ground
15	Overlap TD Veg
16	Overlap HD Ground
17	Overlap HD Veg
18	Overlap Water
19	Overlap Noise

**Table 2 Table of delivered LAS classes combining the hydro (HD) and topo (TD) lidars.**

## 2.5.2 Gridded Surface Models

There are three main data products derived from the lidar point cloud. The first two are based on the elevation and include the Digital Surface Model (DSM) which incorporates valid lidar returns from vegetation, buildings, ground and bathymetry returns, and the Digital Elevation Model (DEM) which incorporates ground returns above and below the water line. The third data product is the intensity of the lidar returns, or the reflectance of the HD lidar. The lidar reflectance, or the amplitude of the returning signal from the HD laser, is influenced by several factors including water depth, the local angle of incidence with the target, the natural reflectivity of the target material, and the voltage or gain of the transmitted lidar pulse. The original data is difficult to interpret because of variances as a result of water depth and loss of signal due to the attenuation of the laser pulse through the water column at different scan angles. The reflectance values were normalized by taking samples of the reflectance values of a common cover type, such as sand, over depth ranges and using these data to establish a relationship between depth and the logarithm of the reflectance value; the inverse of this relationship was used to normalized the data.

## 2.5.3 Aerial Photo Processing

The RCD30 60 MPIX imagery was processed using the aircraft trajectory and direct georeferencing. The low altitude and high resolution of the imagery required that the lidar data be processed first to produce bare-earth digital elevation models (DEMs) that were used in the orthorectification process. The aircraft trajectory, which blends the GPS position and the IMU attitude information into a best estimate of the overall position and orientation of the aircraft during the survey. This trajectory, which is linked to the laser shots and photo events by GPS based time tags, is used to define the Exterior Orientation (EO) for each of the RCD30 aerial photos that were acquired. The EO, which has traditionally been calculated by selecting ground control point (x,y, and z) locations relative to the air photo frame and calculating a bundle adjustment, was calculated using direct georeferencing and exploiting the high precision of the navigation system. The EO file defines the camera position (x,y,z) for every exposure as well as the various rotation angles about the x,y and z axis known as omega, phi and kappa. The EO file along with a DEM can be used with the aerial photo to produce a digital orthophoto. Initially processing was attempted to produce the orthophotos without the lidar DEM. This resulted in orthophotos from adjacent frames not lining up. After the lidar data was processed and classified into ground points, the lidar-derived DEM (above and below the water line) was used in the orthorectification process in Erdas Imagine software and satisfactory results were produced. An example from another mission area of the relative alignment between the photos can be seen in Figure 15. In figure 15, the GPS tripod (yellow legs) is setup over our temporary benchmark. The location of the tripod yellow legs and GPS antenna (white dot) move because of the different perspectives of the photo frames and flight lines. A green triangle has been drawn on the figure to represent the base of the tripod and the green dot represents the GPS benchmark on the ground. These features do not change significantly in the photos from frame to frame demonstrating the accuracy of the resultant orthophotos (Figure 15).

## Little Harbour Ortho Photos: RCD30 Camera Calibration



Figure 15: Example of multiple frames (56, 57, and 58) from multiple flight lines (008 on top and 009 below) of the GPS base station location at Little Harbour after orthorectification. The green dots are GPS locations along the parking lot rail and the aircraft control benchmark on the ground below the tripod where the bottom of the legs are represented by the green diamond.

### 2.5.4 Lidar Validation

Various GPS checkpoints were collected to compare to the lidar points and surface models to ensure the vertical accuracy of the data was sufficient. The GPS elevations were processed to height above chart datum to be consistent with the lidar DEM. These GPS points that represent the bare ground were then overlaid with the lidar DEM and the raster cell value appended to the point file. The difference in elevation between the GPS point and the lidar derived DEM was then computed and summary statistics calculated. The delta Z values, or DZ, can then be displayed graphically on the map. The results of the validation will be shown in the results section.

### 2.5.5 Eelgrass Mapping

The derivation of eelgrass from the lidar data is an active area of research. The eelgrass is dense enough within the bay to affect the elevation of the lidar returns. Although the pulse width of the hydro laser is very small, 4 nsec, and thus is capable of separating targets that are very close in range, such as the water surface and the seabed, it is challenging to map the seabed where dense eelgrass exists. The sensor is utilizing light at 532 nm, there is no ability to “see through”

# PWGSC Bathymetric Lidar Report – Tabusintac, NB

---

the dense eelgrass, and as such, the bathymetry maybe biased to be mapped as being shallower than it is as a result of the eelgrass on the bottom. Similarly, if the eelgrass is so dense that only a single return is detected from the seabed, it is difficult to map the eelgrass based on having multiple returns, where the first or shallowest return is from the eelgrass and the last or deepest return is from the seabed. In addition to analyzing the lidar returns, which are based on range and thus elevation, the other attribute that can be exploited is the seabed reflectance which highlights the seabed cover. The current LSS software does not correct for loss of energy of the signal with water depth, thus the initial reflectance image is not calibrated for depth. We have taken samples of similar seabed cover at different depths and constructed a relationship between depth and reflectance to attempt to compensate for depth. The initial approach to classified eelgrass was designed to exploit the seabed roughness signals derived from the classified seabed lidar bathymetric points. The classified bathymetry points were gridded to a 2 m grid cell resolution taking the maximum elevation of the lidar points within each grid cell. From this bathymetry grid, a slope and aspect grid were constructed. A statistical function using a 3 x 3 cell window was executed on the slope and aspect to calculate the standard deviation of these values within the 3 x 3 kernel. A depth grid was constructed by subtracting the bathymetric grid from a DEM that contained the water surface. The standard deviation of slope and aspect were combined through multiplication and normalized by depth through dividing the product by the depth grid. This produced a grid that represents a range of values based on seabed roughness which is acting as a proxy for eelgrass distribution.

## **3 Results**

The GPS trajectory information for the aircraft has been processed and used in processing the lidar and aerial photography. A seamless Digital Elevation Model has been constructed from a combination of the topo and hydro laser data and orthophotos have been processed from the aerial photographs. An eelgrass presence or absence map has also been constructed from lidar data derivative products.

### **3.1 Lidar Point Cloud Features**

The lidar point cloud was processed in LSS and then further refined in Terrascan. The LAS files from LSS were used to construct project blocks within Terrascan that facilitated the processing and filtering of the data. Various cross-sections of the data were examined in LSS and Terrascan to visualize the point density and classification. In addition to examining the HD laser returns for depth penetration and seabed morphology

### **3.2 Lidar Surface Models**

The classified lidar points were used to construct a variety of lidar surface models. The various models include a continuous Digital Elevation Model (DEM) derived from land to the submerged seabed, a continuous Digital Surface Model that includes trees, buildings, wharves etc. from land to the submerged seabed and a lidar intensity-reflectance map of the seabed cover type.

## 3.2.1 Intensity-Reflectance Data

The lidar intensity-reflectance data is a measurement of the backscatter of the laser returns, and varies according to bottom type (Figure 16). We expect that research into how reflectance is derived from intensity will lead to more advanced algorithms which will allow us to more accurately classify the bottom type as sand, eelgrass, rockweed, etc.

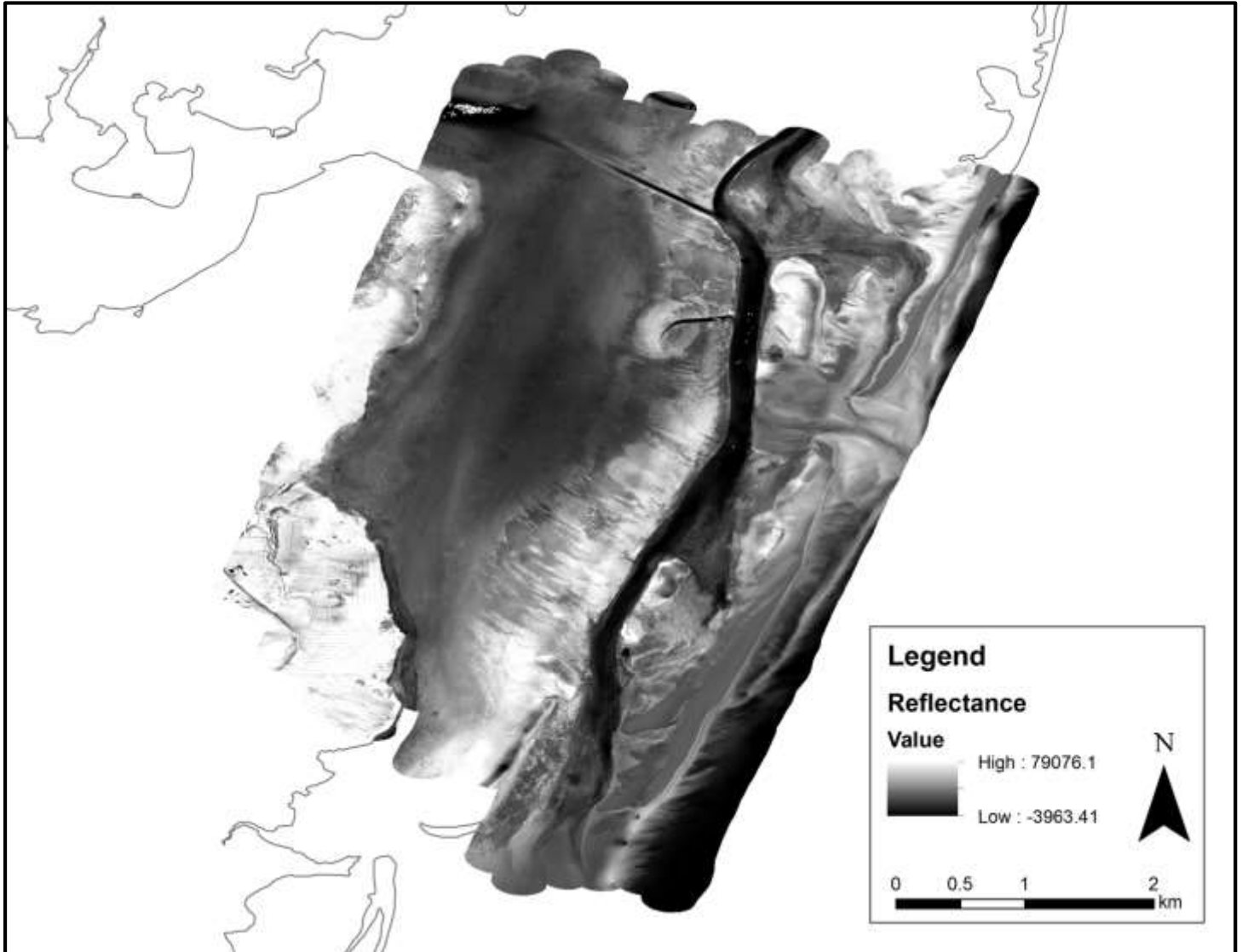


**Figure 16** Example of the green lidar seabed reflectance. High values of reflectance indicate more light is being reflected (less light being absorbed, e.g. bright materials), and low values indicate less light is being reflected (more light being absorbed, e.g. dark materials). Note that this map of reflectance has not been normalized for depth.

The Digital Elevation Model is referenced to chart datum Figure 17.

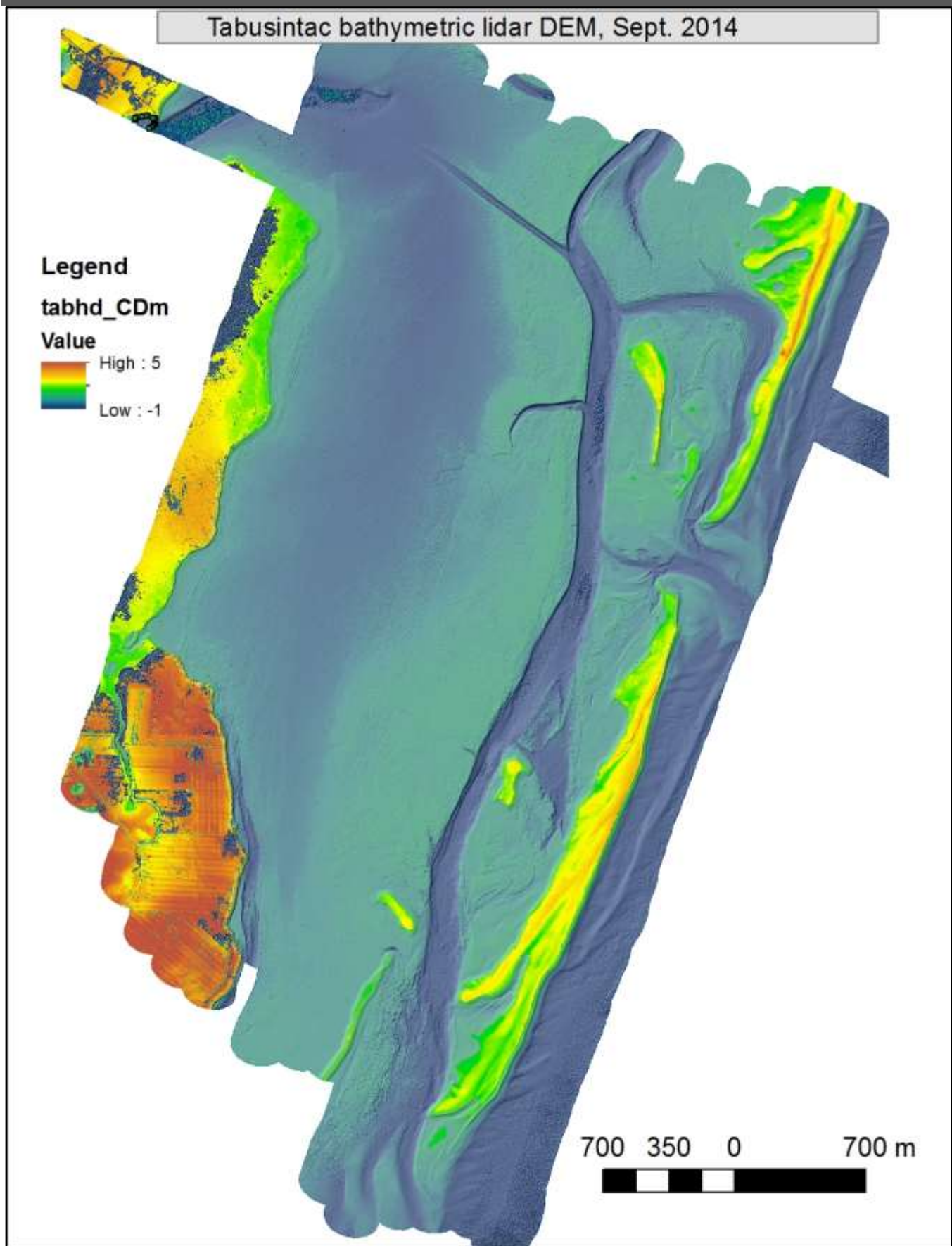


Figure 17 Lidar derived bathymetric map, elevations referenced to chart datum.

## PWGSC Bathymetric Lidar Report – Tabusintac, NB

---

In order to easily interpret the lidar surface models, colour shaded relief (CSR) models were constructed from the DSM for Tabusintac. This map is meant to be for interpretation and is geocoded and compressed in Jpeg 2000 format. If the lidar elevation is required, the lidar DEM or DSM must be used. The CSR map has been colourized to take advantage of Chroma-stereoscopy where the lower elevations are colour coded from the short wavelength blue to higher elevations at longer wavelength red. When the map is viewed with ChromaDepth glasses, it appears in 3-D. The map displays a strong contrast in the physiography and geomorphology of the area, especially in the DEM (Figure 18). The intensity-reflectance was also blended into this map to further enhance the interpretability of the bathymetry and seabed (Figure 19).

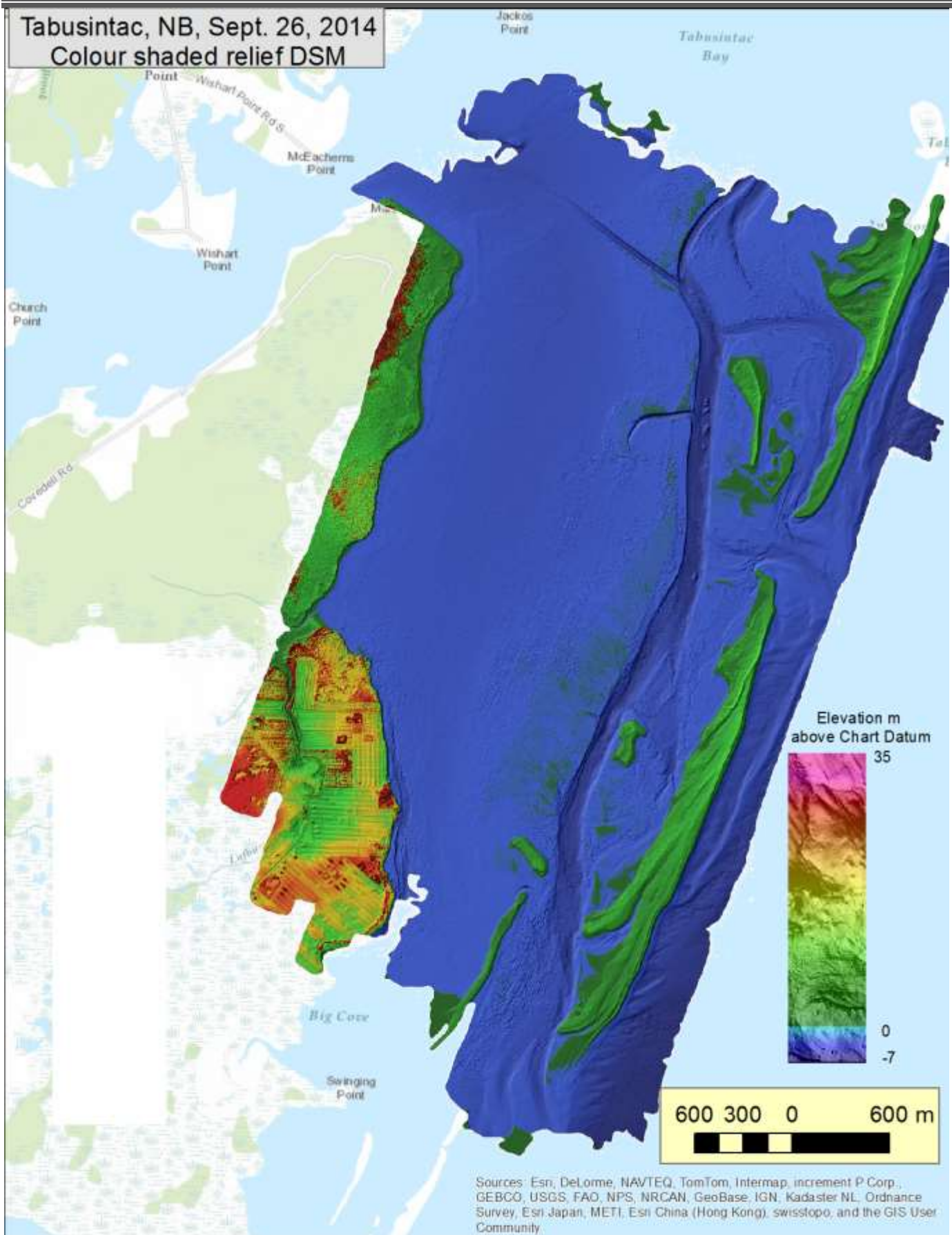


Figure 18 Colour shaded relief map of Tabusintac.

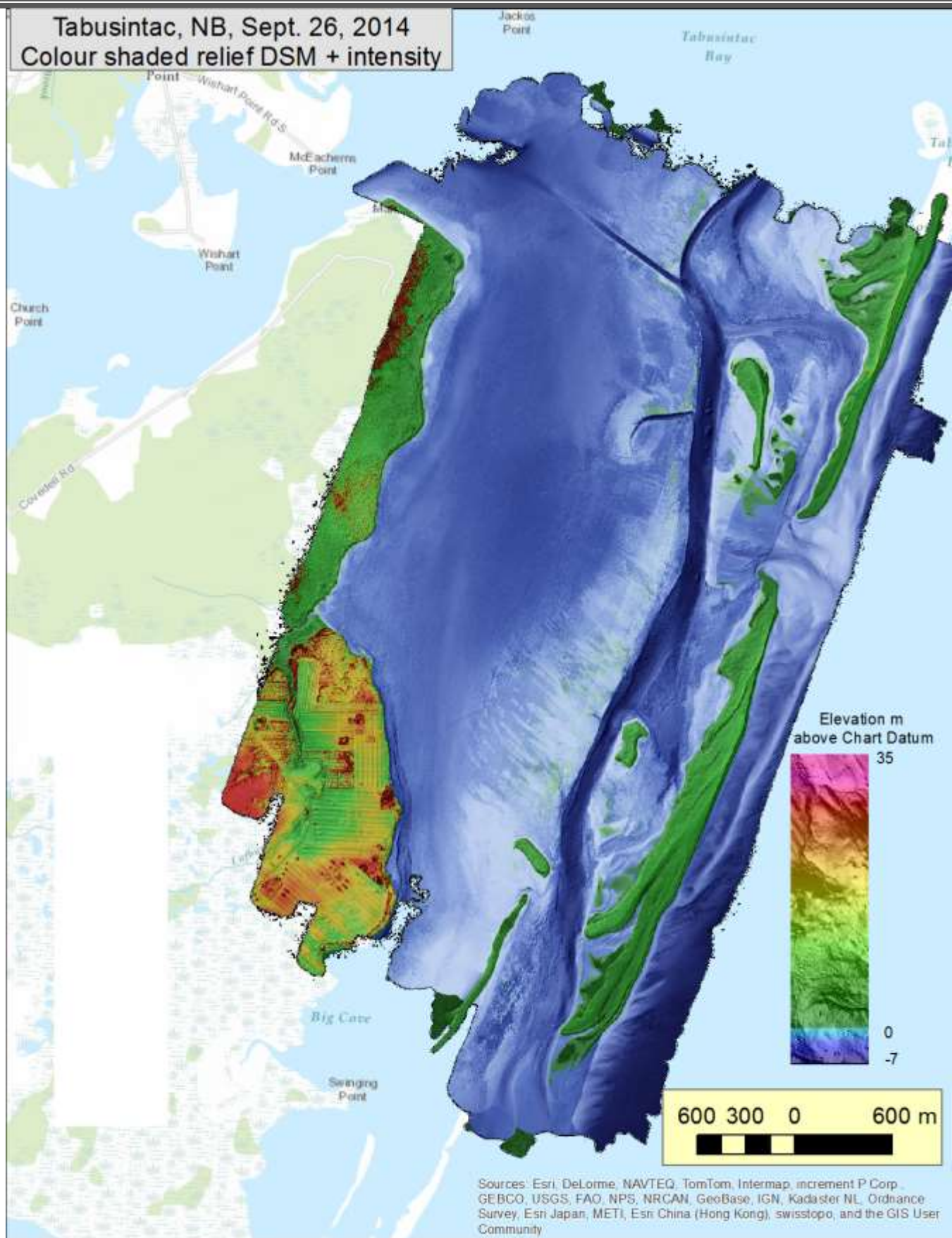


Figure 19 Colour shaded relief with intensity-reflectance map of Tabusintac.

## **3.3 Orthophotography**

The aerial photos for Tabusintac were taken mid-day and the amount of sunlight was not an issue. Photos taken at this time of day, however, have the potential problem of sun glint over the water. The individual orthophotos were used to build a mosaic where the minimum pixel value was selected for the most nadir image to build the mosaic. This resulted in very few areas in the mosaic where sun glint was a problem and the imagery highlights the seabed very well (Figure 20). The RCD30 camera system used to collect the aerial photographs and produce the orthophotos acquired RGB imager (Figure 20) as well as near-infrared (NIR). A colour NIR composite is also presented to highlight this bands sensitivity to vegetation exposed above the water line and to a lesser degree below the water surface (Figure 21). The seabed is visible on the orthophoto mosaic for shallow areas, however it becomes difficult to interpret the cover in deeper parts of the bay.



Figure 20 True colour composite of the Tabusintac orthophoto mosaic.



Figure 21 Colour NIR composite of the orthophoto mosaic of Tabusintac.

### 3.4 GPS Data and Lidar Validation

The GPS base station was a CHS benchmark whose coordinates were provided by PWGSC. As part of the processing, we collected GPS observations from several active control stations in the region during the time of the survey. We used these active control stations to compute the coordinate of the benchmark for future reference and to perhaps establish the chart datum – ellipsoid and geoid relationship. The active control stations included (MIRA, ESCU, OLEA, and RXT2). The results of our processing the coordinates of the benchmark are presented in Table 3.

**Table 3 Computed projection and geodetic coordinates of CHS benchmark.**

				<b>Elevation (m)</b>	
<b>Easting (m)</b> <b>UTM NAD83</b>	351233.384	<b>Northing (m)</b> <b>UTM NAD83</b>	5244833.304	<b>CGVD28</b>	2.44
<b>Longitude</b> <b>(WGS84)</b>	-64° 58' 09.68625''	<b>Latitude</b> <b>(WGS84)</b>	47° 20' 24.14858''	<b>Ellipsoidal</b> <b>WGS84</b>	-17.04

The repetition pulse frequency of the topo laser is much higher than the hydro baser, thus we have a much denser point pattern from the topo laser. This provides extra detail on land but does not add much additional information over the water or for the bathymetry. However, the derived lidar point cloud is a hybrid between the two lidar sensors where the topo lidar is used for points above the water line and the hydro lidar is used for the water surface and bathymetry. The density of the lidar points is demonstrated in Figure 22.



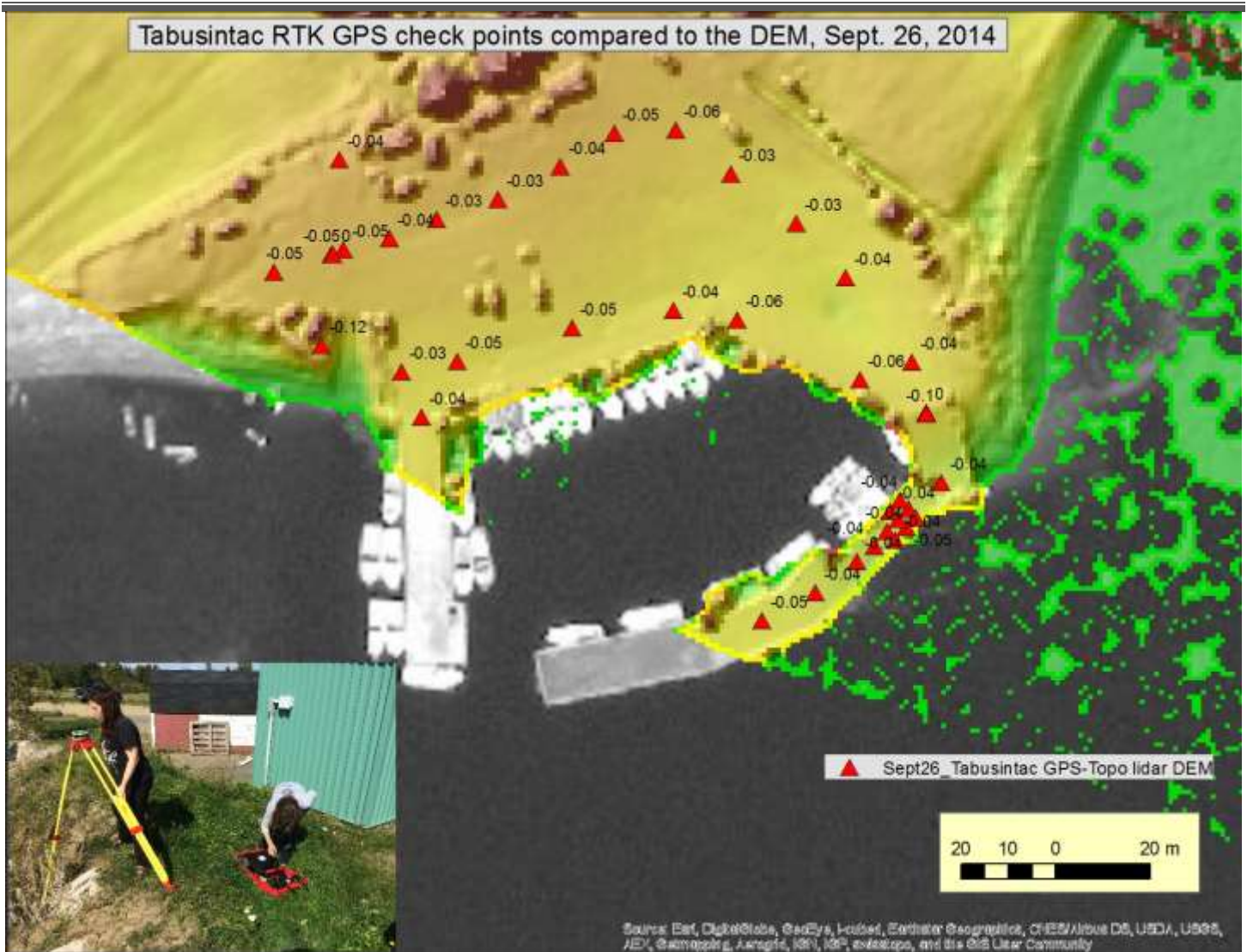


**Figure 23 DEM derived from the topo laser at 2 m grid cells with the RTK GPS checkpoints overlaid (red triangles). The labels indicate the difference in elevation between the GPS and lidar DEM in metres.**

As can be seen in Figure 23 there is good agreement between the GPS check points and the lidar DEM. Figure 24 shows the frequency distribution of the difference in elevation between the GPS and DEM. The majority of the data show a difference very close to zero and are roughly symmetric about zero. The mean difference in elevation is 5 cm with a standard deviation of 2 cm for the 37 checkpoints around the wharf, which were mostly points were collected on hard flat surfaces. In general it appears that the DEM may be too high by 5 cm, although this difference is well within the specifications of the vertical accuracy of the lidar.

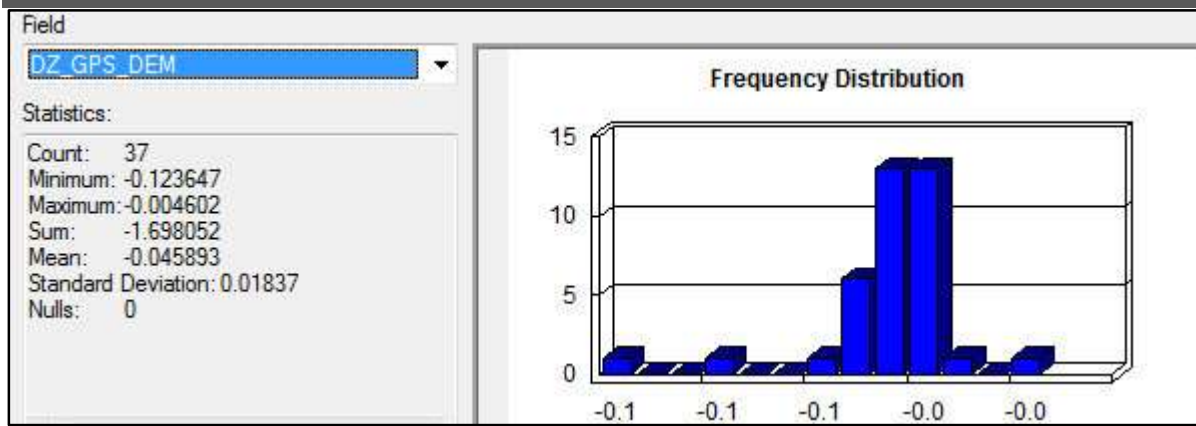


**Figure 24 Histogram of the difference in elevation, DZ, between the GPS checkpoints and the lidar DEM. The mean difference of -0.05 m with a standard deviation of 0.02 m.**

The validation of the depths was accomplished using manual depth measurements and extracting the water surface elevation from the lidar. The depth was then subtracted from the lidar water surface and compared to the lidar elevation model. It should be noted that the horizontal positional accuracy of the depth measurements were based on a code GPS solution which has several metres of uncertainty. Of the 18 seabed computed elevation points the mean difference between them and the lidar seabed elevation was -0.075 m with a standard deviation of 0.26 m. The largest errors appear to be points collected near the channel slope and maybe related to the positional accuracy of the ground truth data (Figure 25).

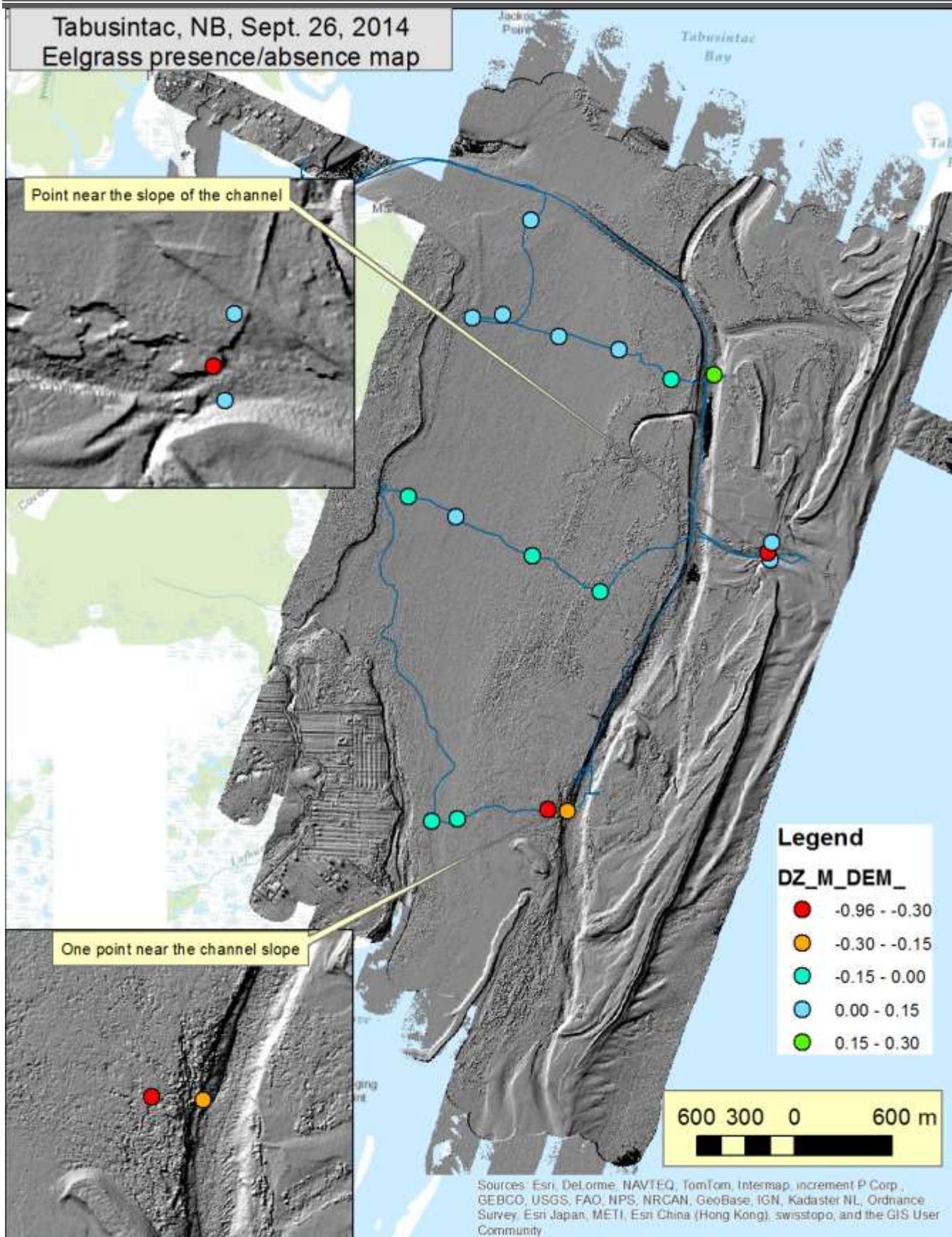


Figure 25 Tabusintac seabed elevation validation. The difference in elevation between the ground truth manual measurements and the lidar elevation is presented in metres as DZ\_m\_DEM.

### 3.5 Eelgrass map

The eelgrass map was derived from the lidar elevation parameters only. The use of the lidar intensity is still an area of research that we feel offers a great deal of potential. However, for this project we exploited the variability in the elevation of the lidar returns where a rougher bottom corresponded to eelgrass compared to a smooth sandy bottom. The map was constructed by combining a variety of lidar elevation derivatives including depth, and the variability of slope and aspect. This produced a map with a range of values representing different levels or probabilities of eelgrass occurrence (Figure 26). This map is compared to the boat based ground truth where the presence or absence of eelgrass has been determined (Figure 27). This map has been further simplified into a presence/absence map for eelgrass (Figure 28) where the ground truth has been plotted and those that match the map are highlighted by a yellow circle. Of the 69 ground truth points, 55 match the map in terms of presence or absence of eelgrass which indicates an 80% agreement.



Figure 26 Eelgrass probability map, darker green indicates a higher probability of eelgrass occurrence.

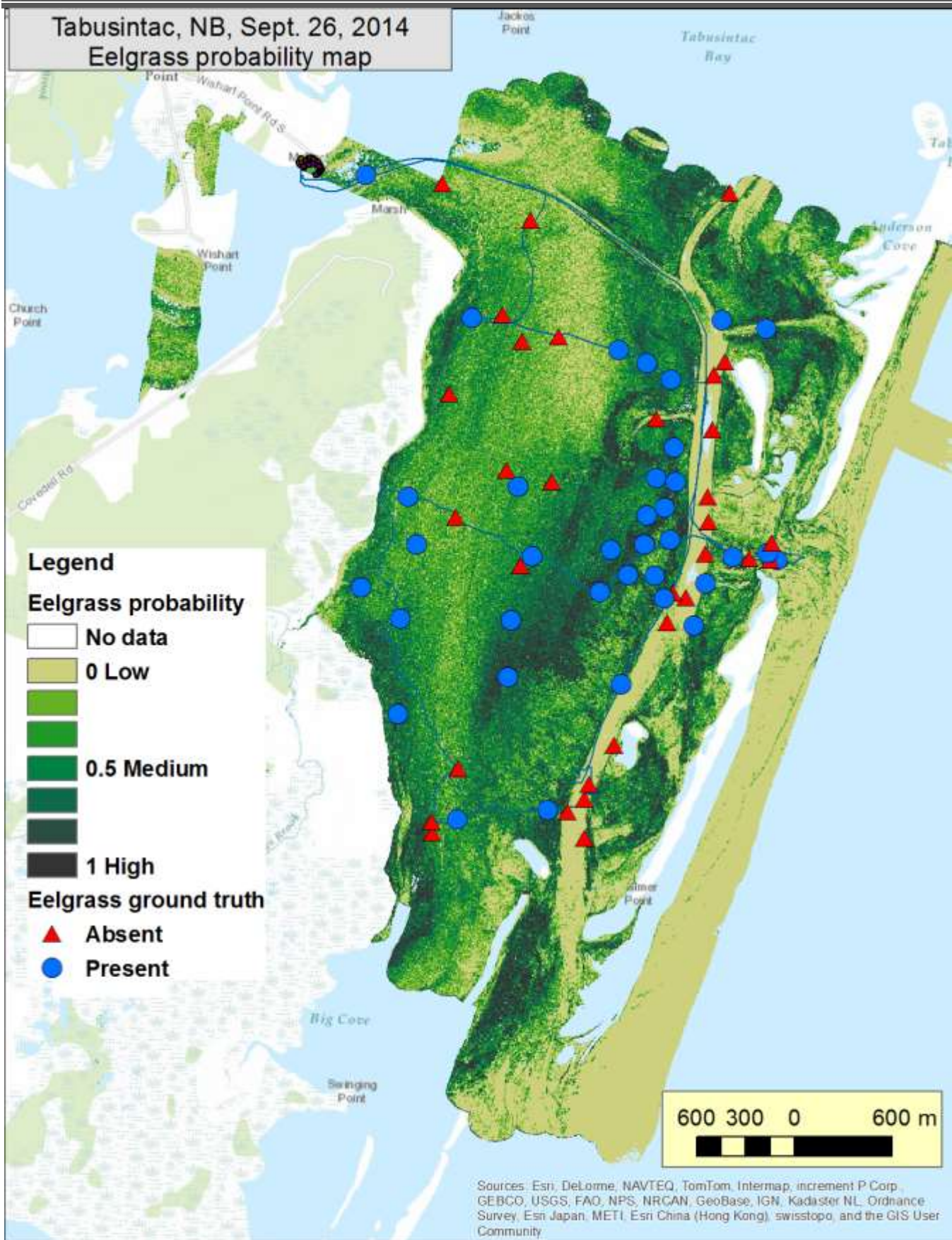


Figure 27 Eelgrass probability map with ground truth, eelgrass presence is a blue dot, absence is a red triangle.

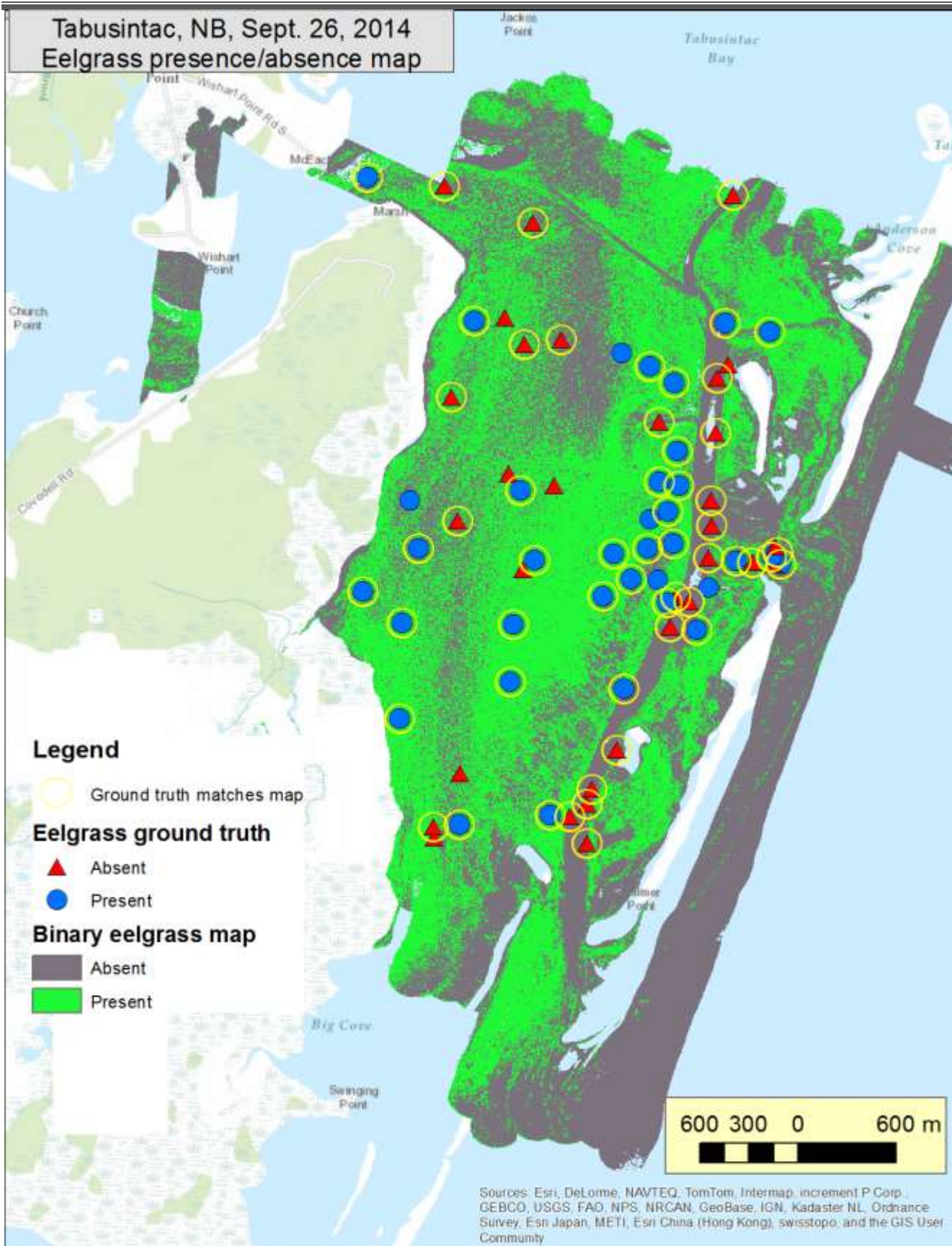
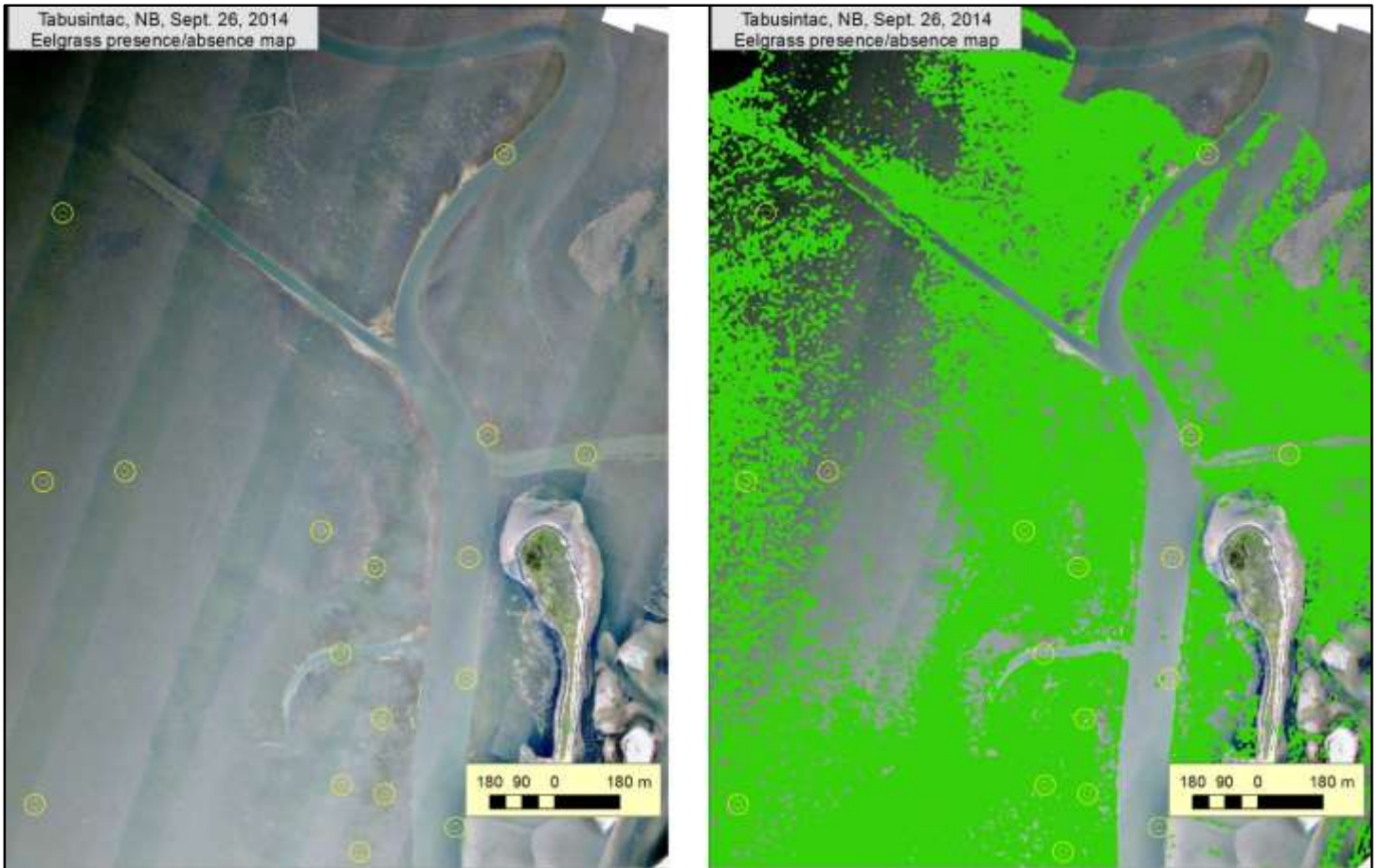


Figure 28 Presence-absence eelgrass map derived from lidar with ground truth (red triangle, blue dot) and where the ground truth matches the map (yellow circles).

## PWGSC Bathymetric Lidar Report – Tabusintac, NB

The orthophoto can be examined in combination with the ground truth and eelgrass map to make a visual assessment. The eelgrass map has been smoothed using a 5 by 5 kernel where the central pixel is replaced with the majority value. The resultant eelgrass presence class has been superimposed over the orthophoto along with the ground truth points that agree with the classification. The extent of the orthophoto is slightly larger than that of the lidar and derived eelgrass map (Figure 29, Figure 30 and Figure 31).



**Figure 29 Orthophoto on the left of the dredged channel with ground truth points that agree with the map. Right is the orthophoto with lidar derived eelgrass (green) and ground truth points.**

## PWGSC Bathymetric Lidar Report – Tabusintac, NB

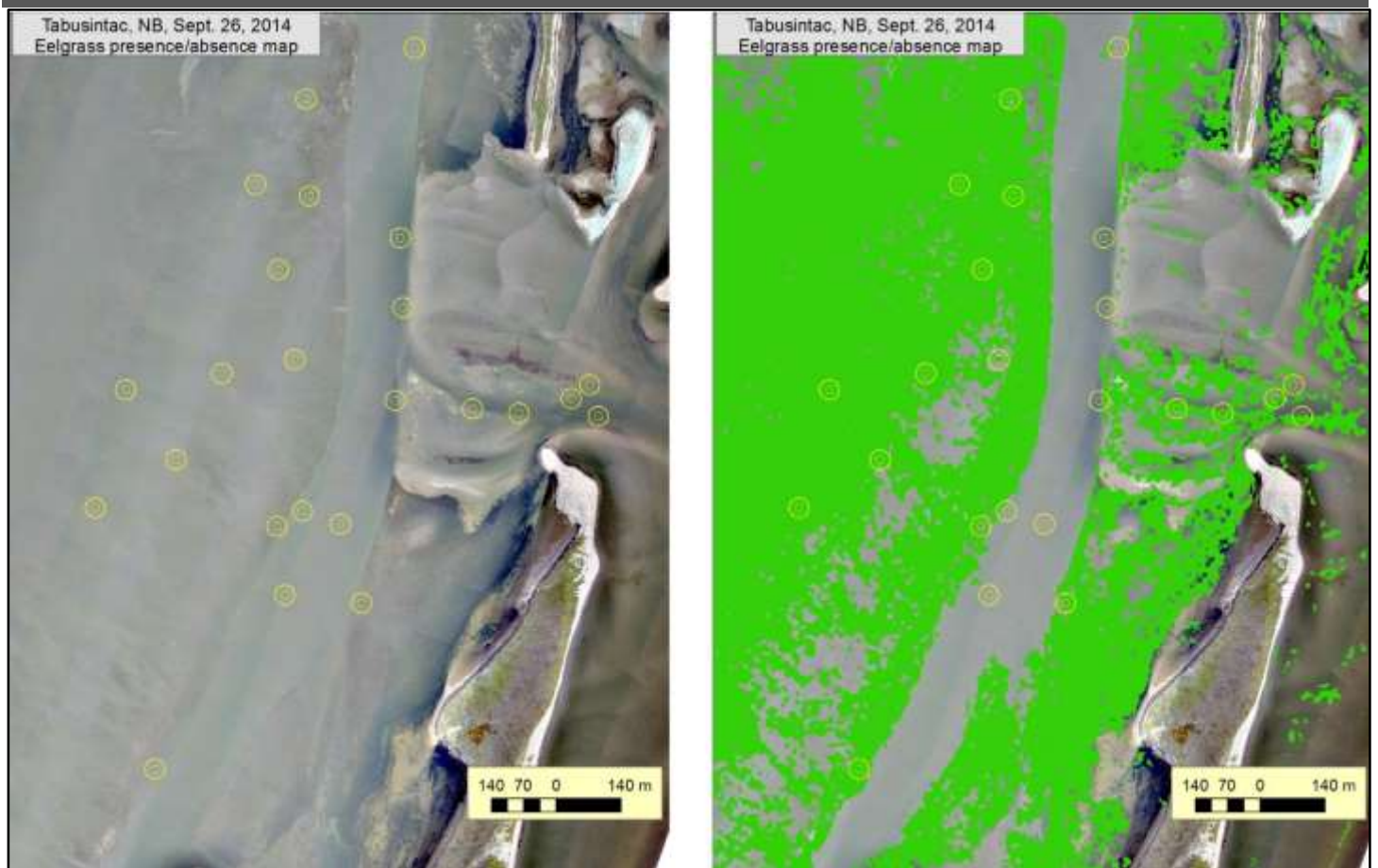


**Figure 30** Orthophoto on the left of the main channel and opening with ground truth points that agree with the map. Right is the orthophoto with lidar derived eelgrass (green) and ground truth points.

## PWGSC Bathymetric Lidar Report – Tabusintac, NB

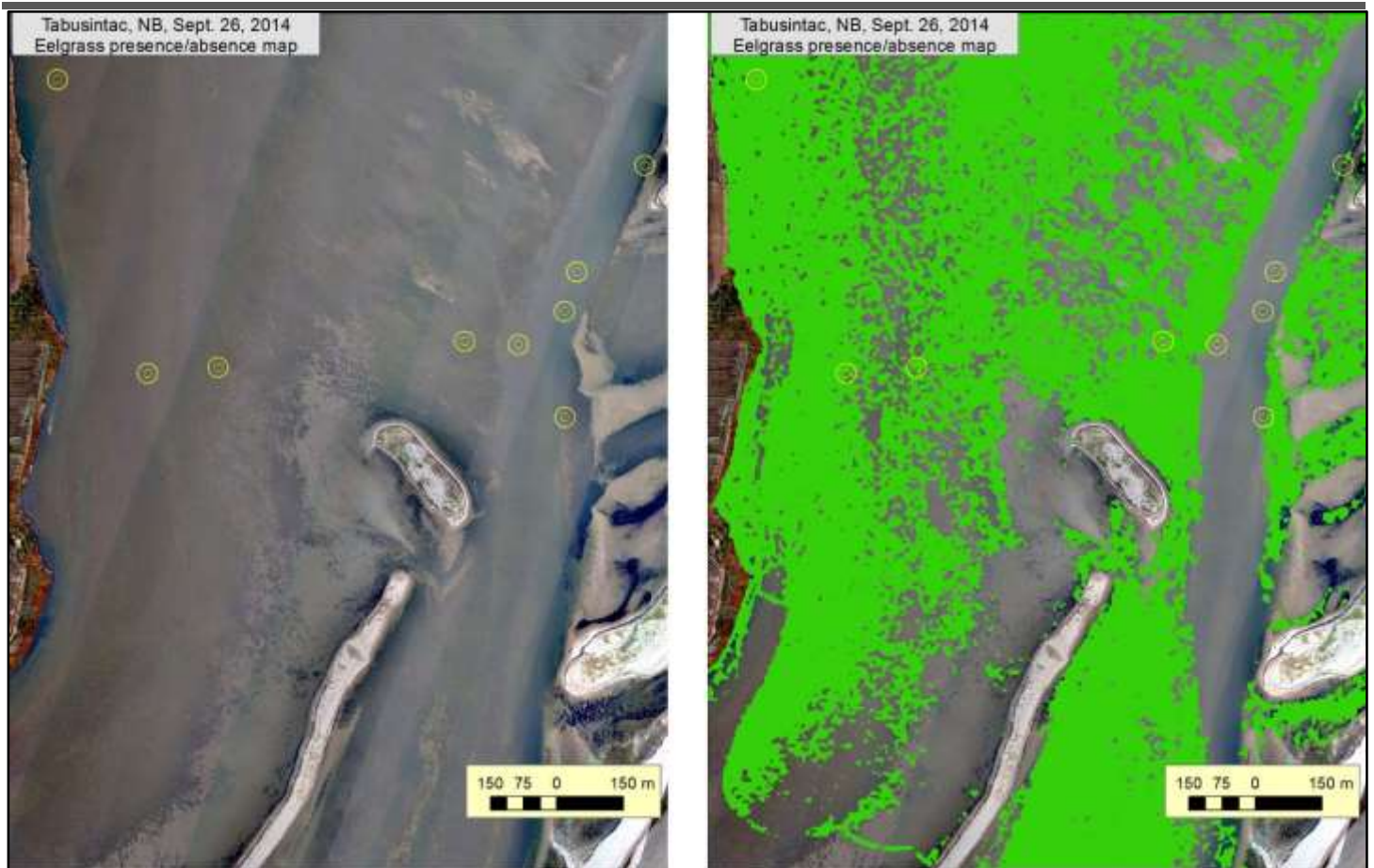


**Figure 31 Orthophoto on the left of the southern channel with ground truth points that agree with the map. Right is the orthophoto with lidar derived eelgrass (green) and ground truth points.**

### 4 Conclusions

The inaugural mission of the new NSCC topo-bathy lidar sensor, Chiroptera II, was a huge success with nearly 100% complete data collection in the study area. Researchers at AGRG learned many valuable lessons about the operations of the sensor and the variability of local environmental conditions that affect water clarity, a major factor influencing the success of a near shore bathymetric lidar survey. An extensive ground truth campaign was mobilized for the surveys from scientists at AGRG and DFO Gulf Region and supplemented by staff from Stantec for another project near the time of the survey. The lidar provided unprecedented detail on the bathymetry of the bay, although dense eelgrass has probably biased the elevation of the seabed to be mapped at a higher elevation than it is. The validation of the lidar at the wharf has indicated it is extremely accurate. Limited validation data were available to test the bathymetry. The ground truth data and the derived lidar map products were used to develop a method to classify the presence and absence of eelgrass. Comparison between the ground truth and this map indicates an 80% agreement. The production of a normalized lidar reflectance map allows the seabed cover to be interpreted and compared to information visible from the orthophoto mosaic and the eelgrass map. The reflectance was not used in the production of the eelgrass map, although it is an area that AGRG plans to continue to research how it can be best used and believes valuable information on the seabed can be

## PWGSC Bathymetric Lidar Report – Tabusintac, NB

---

derived from it. The detail of the topo and hydro lasers provide a rich dataset that many different users can access and derive information from including general mapping, coastal processes, coastal vulnerability assessment, and fisheries and aquaculture development to name a few. The detailed bathymetry reveals new insights into the near shore topography and surficial geology that may pose navigation hazards, as well as the distribution of sand deposits and submerged vegetation. These data provide a rich environment for future studies of coastal processes and have the potential to advance our knowledge and improve coastal development in a responsible and sustainable way. The processing of the high resolution photographs into an orthophoto mosaic provides additional data that can be compared to the lidar maps. We will continue to actively research new methods to derive a seabed cover classification from the lidar derivatives that include the reflectance data and expect the accuracy of eelgrass mapping to improve in the future.

Various datasets have been delivered with this project including the lidar point data both in LAS format as well as simple ASCII. In addition to the point data, various raster surface models have been derived from the lidar data and are in GeoTif format. They consist of rasters representing different elevation surfaces, for example the bare-earth land and bathymetry, or the water surface, where all of the elevations are referenced to local chart datum. An additional raster surface has been constructed for the seabed that represents the reflectance from the hydro green laser. Two eel grass maps have been delivered in raster GeoTif format in the EELGRASS directory, eelg\_revised\_fnl has two classes that represent eelgrass presence or absence as derived from the lidar, and eelgrass\_present is a binary map that only has a class where eelgrass is present. Three types of validation were conducted in this study; 1) a comparison of elevation between the lidar and RTK GPS around the wharf; 2) a depth comparison between AGRG manual measurements of water depth during the survey and those derived from the lidar; and 3) a comparison between the combined ground truth data of eelgrass from DFO, AGRG and Stantec researchers with the eelgrass presence or absence map. The shape files that represent these data are located in the VALIDATION directory are named : Sept26\_Tabusintac\_GPS\_CD\_TD, depth\_validation, and Combined\_eelgrass\_Tabusintac respectively. In the case of elevation and depth the lidar surf ace model elevation has been subtracted from the control data (GPS or manual depth measurements) to calculate a delta Z value. In the case of the eelgrass ground truth the value of the presense-absense map has been appended to the ground truth point file for comparison.